IEEE Access
Multidisciplinary | Rapid Review | Open Access Journal

Received May 22, 2019, accepted June 4, 2019, date of publication June 7, 2019, date of current version June 26, 2019.

Digital Object Identifier 10.1109/ACCESS.2019.2921545

A Novel Hybrid Harris Hawks Optimization for Color Image Multilevel Thresholding Segmentation

XIAOLI BAO, HEMING JIA, (Member, IEEE), AND CHUNBO LANG
College of Mechanical and Electrical Engineering, Northeast Forestry University, Harbin 150040, China

Corresponding author: Heming Jia (jiaheming@nefu.edu.cn)

This work was supported in part by the Fundamental Research Funds for the Central Universities under Grant 2572019BF04 and in part by the Northeast Forestry University Horizontal Project under Grant 43217002, Grant 43217005, and Grant 43219002.

ABSTRACT Multilevel thresholding has got more attention in recent years with various successful applications. However, the implementation becomes more and more complex and time-consuming when the number of thresholds is high, and color images which contain more information are even worse. Therefore, this paper proposes an alternative hybrid algorithm for color image segmentation, the advantages of which lie in extracting the best features from the high performance of two algorithms and overcoming the limitations of each algorithm to some extent. Two techniques, Otsu's method, and Kapur's entropy, are used as fitness function to determine the segmentation threshold values. Harris hawks optimization (HHO) is a novel and general-purpose algorithm, and the hybridization of HHO is fulfilled by adding another powerful algorithm—differential evolution (DE), which is known as HHO-DE. More specifically, the whole population is divided into two equal subpopulations which will be assigned to HHO and DE algorithms, respectively. Then both algorithms operate in parallel to update the positions of each subpopulation during the iterative process. In order to fully demonstrate the superior performance of HHO-DE, the proposed method is compared with the seven state-of-the-art algorithms by an array of experiments on ten benchmark images. Meanwhile, five measures, including the average fitness values, standard deviation (STD), peak signal to noise ratio (PSNR), structure similarity index (SSIM), and feature similarity index (FSIM), are used to evaluate the performance of each algorithm. In addition, Wilcoxon's rank sum test for statistical analysis and the comparison with the super-pixel method are also conducted to verify the superiority of HHO-DE. The experimental results reveal that the proposed method significantly outperforms other algorithms. Hence, the HHO-DE algorithm is a remarkable and promising tool for multilevel thresholding color image segmentation.

INDEX TERMS Image segmentation, hybrid algorithm, Harris hawks optimization, differential evolution, Kapur's entropy, Otsu's method.

I. INTRODUCTION

Image segmentation is a vital preprocessing stage in object recognition and robotic vision, and has drawn an increasing attention in recent years [1]. This work is dedicated to partition a given image into several non-overlapping subregions with respect to feature, color, texture, etc., which in turn helps to extract the interested objects or meaningful contours. More specifically, the grey values of pixels show similarity in the same region, whereas the grey value varies from pixel to pixel among different regions [2]. Nowadays, image segmentation technique has been widely used in all kinds of fields, such as precision husbandry [3], medical diagnosis [4], digital rock physics [5]. Moreover, many scholars are unceasingly promoting the research of image segmentation ahead.

In the last few years, a great variety of methods have been proposed to enrich image segmentation technique, which can be divided into four types: region-based method, clustering-based method, graph-based method, and thresholding-based method [6]–[8]. Among the existing methods, thresholding technique based on gray level histogram has become the most popular with its high accuracy

The associate editor coordinating the review of this manuscript and approving it for publication was Orazio Gambino.

and simple implementation [7]. The kernel is that the pixels will be divided into different classes through comparison between threshold values and their own intensity levels. If the objects and background can be separated using a single threshold value, it is known as bi-level segmentation. However, it is necessary to divide an image into several different classes using multiple threshold values in the majority of cases, which is termed as multilevel segmentation [9], [10]. Besides, numerous techniques based on respective predefined criteria have been proposed for selecting appropriate thresholds during the last couple of decades [11], such as, Otsu's method [12], Kapur's entropy [13], minimum cross entropy [14], fuzzy entropy [15], and Tsallis entropy [16]. Among them, Otsu's method and Kapur's entropy are the most popular ones due to simplicity and efficiency [17]. Otsu's technique maximizes the between class variance of each segmented class to obtain the optimal thresholds, and Kapur's technique measures the homogeneity between classes by maximization of the histogram entropy. However, these classical methods perform good capability only in the case of a lower threshold level. When the number increases, the computational time will present exponential growth [18]. Therefore, further researches that made creative use of meta-heuristic algorithms are proceeding to reduce the time complexity and maintain image segmentation accuracy.

The segmentation of each image can be considered as a specific optimization problem under certain constraints [19], the aim of which is to find more realistic and feasible solutions. Meta-heuristic algorithms inspired by nature with respective unique global and local searching strategies, have been effectively applied to the optimization field [20], [21]. For instance, dragonfly algorithm (DA) inspired from the static and dynamic behaviors of dragonflies, has been applied in optimization of proportional-integral-derivative (PID) controller [22]; whale optimization algorithm (WOA) inspired by the foraging behavior of humpback whales, has been used to extract the parameters of solar photovoltaic (PV) models [23]; Moth search algorithm (MSA) which imitates the phototaxis and levy flight of the moths, can be applied to solve cloud task scheduling problems effectively [24]. Better yet, the application of meta-heuristic algorithms has been extensive in the domain of multilevel thresholding image segmentation. For example, He and Huang proposed a modified firefly algorithm (MFA) based on the processing of mutual attraction and movement in the swarm for color image segmentation, using between-class variance, Kapur's entropy, and minimum cross entropy techniques [25]; Khairuzzaman and Chaudhury presented the grey wolf optimizer (GWO) using the Otsu's method and Kapur's method for image segmentation [26]; Shen *et al.* [27] demonstrated the validity of modified flower pollination algorithm (MFPA) by an array of experiments on real-life images and remote sensing images segmentation.

Any meta-heuristic algorithm is imperfect and has its own limitations which affect the performance. Hence, a number of strategies have been propounded to overcome these weaknesses. Hybridization is a better and more remarkable choice among them [28], in which some individuals are combined with different operators to obtain superior results. What is worth mentioning, recently several hybrid swarm algorithms have been effectively applied for image segmentation. For example, the gravitational search algorithm (GSA) combined with genetic algorithm (GA) showed excellent segmentation performance in both between-class variance and entropy criteria [29]; the hybridization between whale optimization algorithm (WOA) and particle swarm optimization (PSO) can reduce the computational complexity without affecting the accuracy of multilevel thresholding [30].

This paper presents an efficient alternative hybrid algorithm for multilevel thresholding image segmentation by combining the HHO and DE. The HHO is a novel swarm algorithm which was proposed in 2019 by Heidari [31]. It is inspired from the cooperative behavior and chasing style of Harris hawks. Similar to other meta-heuristic algorithms, the HHO also contains the phases of exploration and exploitation. The hawks will perch randomly on some locations for monitoring various regions, so as to track and detect the rabbit during the exploration stage. Whereas the hawks will conduct surprise pounce or team rapid dives to exploit the neighborhood of intended prey in the stage of exploitation. Its advantages include high-quality solutions, strong robustness, and smooth transition between exploration and exploitation [31]. Moreover, the HHO algorithm shows superior performance in real-world engineering problems, including three-bar truss design problem, tension spring design, pressure vessel design problem, welded beam design problem, and multi-plate disc clutch brake [31]. On the other hand, DE is a classical and powerful algorithm, which has been used in order management [32], robot navigation [33], synthetic inertia control [34], and other fields. In addition, DE has also became more and more popular in hybrid algorithms for image segmentation in recent years, and an array of experiments significantly verify its advantages. For example, the hybridization of differential evolution (DE) algorithm is done by adding the reset tactics adopted from the Cuckoo Search (CS) algorithm [35], the results reveal the superiority of this hybrid algorithm in image thresholding.

A prime motivation for this article is to obtain the optimum thresholds for color image segmentation based on the hybridization of HHO and DE algorithm. The proposed method not only extracts the best features from the high performance of two algorithms, but also overcomes the limitations of HHO and DE algorithm to some extent. The process of implementation as follows: firstly, all individuals are divided into two equal subpopulations according to fitness function values, which will be assigned to Harris hawks swarm and DE algorithm respectively. Then the HHO and DE algorithms perform in parallel to update the positions of each subpopulation. Finally, the two updated subpopulations are merged together to generate a new population and the global solution is selected from it.

It is evident that color images contain more information compared with gray images, highlighting the difficulty of color image segmentation. With powerful optimizing ability, high accuracy, strong robustness and remarkable stability, the proposed method can accomplish complex task of color image segmentation so well. In this paper, between-class variance and Kapur's entropy are used as objective functions which will be maximized to find the optimal thresholds. Several state-of-the-art meta-heuristic algorithms are selected for comparison, such as the standard HHO [31], DE [35], sine cosine algorithm (SCA) [36], bat algorithm (BA) [37], harmony search optimization (HSO) [38], PSO [39], and dragonfly algorithm (DA) [40]. Furthermore, five indicators, the average fitness values, STD, PSNR, SSIM, and FSIM, are chosen as quality metrics to compare the performance of proposed algorithm with other algorithms. Wilcoxon's rank sum test [41] is also performed to verify the superiority of HHO-DE in a statistical way. Moreover, the performance of proposed method is compared with super-pixel approach to verify its practicability.

The goals of this paper are as follows:

1. An improved HHO method, HHO-DE, is proposed for multilevel image thresholding task. HHO-DE, based on the hybridization with DE algorithm, combines the merits of two algorithms meanwhile avoids the respective limitations through divide the population into two subpopulations, and thereby make a better balance between exploration and exploitation.

2. HHO-DE algorithm is applied to the process of optimal thresholds for multilevel image segmentation. Multiple performance aspects including solution quality, segmentation accuracy, convergence property, robustness, statistics, and stability are evaluated to comprehensively verify the effectiveness of HHO-DE.

3.The performance of HHO-DE is extensively compared with seven state-of-the-art meta-heuristic algorithms. The comparison results consistently demonstrate that HHO-DE is highly competitive and can be used as an effective alternative for color image segmentation.

The reminder of this paper is organized as follows: Section II introduces Otsu's method and Kapur's entropy techniques for multilevel thresholding briefly. Section III gives an overview of Harris hawks optimization Section IV describes the hybrid algorithm for multilevel thresholding color image segmentation. Section V presents a description of experiment in detail. Subsequently, the experimental results of proposed algorithm compared to other algorithms and its analysis in terms of six indicators are discussed in Section VI. Finally, the conclusion is illustrated in Section VII.

II. MULTILEVEL THRESHOLDING

In this section, we introduce two most widely used image thresholding techniques, including Otsu's method which is based on between class variance and Kapur's method which is based on the criterion of entropy. There are two categories in image segmentation: bi-level and multilevel. We will provide a brief formulation in the following subsections.

A. OTSU METHOD

Otsu method selects the optimum values of thresholds by maximizing between class variance of each segmented class [9]. It can be defined as follows: assume that L denotes the number of gray levels in a given image so that the range of intensity values is $[0, L-1]$. N is the total number of pixels, and then n_i represents the number of pixels in which gray level is i

$$N = \sum_{i=0}^{L-1} n_i \tag{1}$$

The probability of each gray level i is calculated as follows:

$$p_i = \frac{n_i}{N} \ (p_i \geq 0) \tag{2}$$

The optimum threshold t partitions the given image into two classes, namely, foreground and background, which can be described as follows:

$$\begin{cases} D_1 = \{g(x,y) \,|0 \leq \mathrm{g}(x,y) \leq t\} \\ D_2 = \{g(x,y) \,|t+1 \leq \mathrm{g}(x,y) \leq L-1\} \end{cases} \tag{3}$$

The between class variance of two regions can be described using the following equation:

$$\sigma_B^2(t) = P_0 \times (m_0 - m_G)^2 + P_1 \times (m_1 - m_G)^2 \tag{4}$$

where

$$P_0 = \sum_{i=0}^{t} p_i \quad P_1 = \sum_{i=t+1}^{L-1} p_i$$

$$m_0 = \frac{1}{P_0} \sum_{i=0}^{t} i p_i \quad m_1 = \frac{1}{P_1} \sum_{i=t+1}^{L-1} i p_i$$

$$m_G = \sum_{i=0}^{L-1} i p_i$$

P_0 and P_1 denote the cumulative probabilities of foreground and background respectively. m_0 and m_1 represent the mean level of two classes respectively. m_G is the mean level of given image.

(4) is maximized to obtain the optimal threshold t^* for image segmentation which is formulated by:

$$t^* = \underset{0 \leq t \leq L-1}{\arg} \max\left(\sigma_B^t(t)\right) \tag{5}$$

Furthermore, Otsu's method can be effectively extended for multilevel thresholding problems. Assume that the given image is subdivided into n classes so that there are $n-1$ optimal thresholds, through maximization of the objective function. These classes are described by:

$$\begin{cases} D_0 = \{g(x,y) \,|0 \leq \mathrm{g}(x,y) \leq t_1 - 1\} \\ D_1 = \{g(x,y) \,|t_1 \leq \mathrm{g}(x,y) \leq t_2 - 1\}, \cdots \\ D_i = \{g(x,y) \,|t_{i-1} \leq \mathrm{g}(x,y) \leq t_i - 1\}, \cdots \\ D_{n-1} = \{g(x,y) \,|t_{n-2} \leq \mathrm{g}(x,y) \leq t_{n-1} - 1\} \end{cases} \tag{6}$$

The cumulative probabilities of each class are calculated by:

$$P_k = \sum_{i=T_k}^{T_{k+1}-1} p_i \, (k = 0, 1, \cdots, n-1) \tag{7}$$

The mean levels of each class are defined as follows:

$$\mu_k = \frac{1}{P_k} \sum_{i=T_k}^{T_{k+1}-1} i p_i \, (k = 0, 1, \cdots, n-1) \tag{8}$$

The mean level of whole image is defined as follows:

$$\mu = \sum_{i=0}^{L-1} i p_i \tag{9}$$

The objective function based between-class variance is calculated by:

$$\sigma_B^2 \, (t) = \sum_{k=0}^{n-1} P_k \, (\mu_k - \mu)^2 \tag{10}$$

Note that, $P_k \, (\mu_k - \mu)^2$ shows the difference between μ_k and the mean intensity in the whole image that weighed by P_k. The optimum thresholds $t^* \left(t_1, t_2, \cdots t_n\right)$ are obtained by maximizing the between-class variance objective function [42]. A higher value of objective function refers to better quality of the segmented images.

B. KAPUR'S ENTROPY

The Kapur's method is used to determine the optimal threshold values through the maximization of Kapur's entropy. It has attracted the interests of a lot of researchers because of its superior performance, and has been widely applied to solve image segmentation problems. The entropy of a given image represents the compactness and separateness among distinctive classes [43].

Let N be the number of pixels and L be the number of levels in a given image. We can describe the probability p_i of each gray level i as follows:

$$p_i = \frac{h_i}{\sum_{i=0}^{L-1} h \, (i)} \tag{11}$$

where h_i denotes the number of pixels with gray level i

For bi-level thresholding, the Kapur's entropy objective function is defined using the following equation:

$$f \, (t) = H_0 + H_1 \tag{12}$$

where

$$H_0 = -\sum_{t=0}^{t-1} \frac{p_i}{\omega_0} \ln \frac{p_i}{\omega_0}, \quad \omega_0 = \sum_{i=0}^{t-1} p_i$$
$$H_1 = -\sum_{i=t}^{L-1} \frac{p_i}{\omega_1} \ln \frac{p_i}{\omega_1}, \quad \omega_1 = \sum_{i=t}^{L-1} p_i$$

The Kapur's method finds the optimal threshold t^* by maximizing the objective function, that is

$$t^* = \arg \max_{0 \le t \le L-1} (f \, (t)) \tag{13}$$

The Kapur's method can be also extended to multi-level thresholding, it can be formulated as follow:

$$f \, (t_1, t_2, \ldots\ldots t_n) = H_0 + H_1 \ldots\ldots + H_n \tag{14}$$

where

$$H_0 = -\sum_{t=0}^{t_1-1} \frac{p_i}{\omega_0} \ln \frac{p_i}{\omega_0}, \quad \omega_0 = \sum_{i=0}^{t_1-1} p_i$$
$$H_1 = -\sum_{i=t_1}^{t_2-1} \frac{p_i}{\omega_1} \ln \frac{p_i}{\omega_1}, \quad \omega_1 = \sum_{i=t_1}^{t_2-1} p_i$$
$$H_2 = -\sum_{i=t_2}^{t_3-1} \frac{p_i}{\omega_2} \ln \frac{p_i}{\omega_2}, \quad \omega_2 = \sum_{i=t_2}^{t_3-1} p_i \cdots$$
$$H_n = -\sum_{i=t_n}^{L-1} \frac{p_i}{\omega_n} \ln \frac{p_i}{\omega_n}, \quad \omega_n = \sum_{i=t_n}^{L-1} p_i$$

The optimal thresholds are found by maximizing the objective function, that is:

$$t^* = \arg \max_{0 \le t \le L-1} (f \, (t_1, t_2, \ldots\ldots t_n)) \tag{15}$$

However, the foremost restriction between Otsu's and Kapur's methods is that the computational time is increasing exponentially as the number of thresholds increases. Hence, it is time-consuming practically for multilevel image segmentation applications. In order to overcome the above shortcomings, this paper presents a novel method based on the hybrid Harris hawks optimization algorithm to find optimal thresholds. The purpose of proposed method is to find the optimal thresholds accurately using Otsu's and Kapur's techniques in less processing time.

III. HARRIS HAWKS OPTIMIZATION

Study author Heidari modeled the unique cooperative behaviors of Harris hawks mathematically to propose a novel stochastic metaheuristic, namely, the HHO algorithm which can be used to address a variety of optimization problems [31]. The behavior characteristic of Harris hawks is that they trace, encircle, approach, and finally attack the potential prey (rabbits in most cases) by means of good teamwork. A skillful manoeuvring called ''surprise pounce'' will be effectively carried out in hunting escaping preys. The concrete implementing process of surprise pounce is: team members make active attacks from different directions respectively and then converge to the intended rabbit. A switch strategy—the chase will go on under the leadership of another team member, aims to perplex the escaping rabbit when the best hawks comes straight towards the rabbit and gets lost. Similar to other meta-heuristic algorithms, the HHO algorithm also contains the phases of exploration

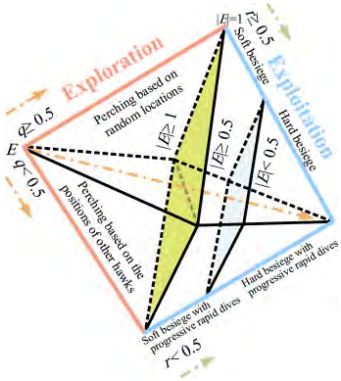

FIGURE 1. Different phases of Harris hawks optimization [31].

and exploitation. The hawks will perch randomly on some locations for monitoring various regions, so as to track and detect the rabbit during the exploration stage. Whereas the hawks will conduct surprise pounce or team rapid dives to exploit the neighborhood of intended prey in the stage of exploitation. The positions of hawks are considered as candidate solutions. The best position of is defined as the intended rabbit location. Fig. 1 shows all phases of HHO algorithm, which will be introduced at length in the following subsections.

A. EXPLORATION PHASE

In this phase, Harris hawks update their position through two tactics, and both have the equal probability to be chosen. Which can be described in detail as follows: A random value of $p < 0.5$ means the hawks perch on some locations according to the position of other team members, and the position of each hawk is updated by (16). In this way, all members can ensure to be close enough when attacking the intended prey. On the other hand, a random value of $p \geq 0.5$ indicates that the hawks perch on giant trees randomly to explore the desert site, and the population using the (17) to update positions.

$$X(t+1) = \left(X_{prey}(t) - X_m(t)\right) - r_3\left(LB + r_4 \Delta B\right) \quad (16)$$

$$X(t+1) = X_{rand}(t) - r_1 \left|X_{rand}(t) - 2r_2 X(t)\right| \quad (17)$$

where $X(t+1)$ is the position vector of hawks in the next iteration. $X_{prey}(t)$ represents the position of intended rabbit. $X_{rand}(t)$ is the position of a hawk which is chosen randomly from current team. r_1, r_2, r_3 and r_4 are random numbers, which can provide more diversification trends and make sure the hawks explore different regions of the search space. $\Delta B = UB - LB$, UB and LB are the upper and lower bounds of search space. t is the current iteration counter. And $X_m(t)$ is the average position of the current population of hawks which is calculated by the following equation.

$$X_m(t) = \frac{1}{N}\sum_{i=1}^{N} X_i(t) \quad (18)$$

where $X_i(t)$ represents the position of each hawk. N indicates the total number of team members.

B. TRANSITION FROM EXPLORATION TO EXPLOITATION

As the intended prey try to run away from the attack, the retained energy of prey constantly decreases, which can be modeled as follows:

$$E = 2E_0\left(1 - \frac{t}{T}\right) \quad (19)$$

where E_0 ranged from -1 to 1 denotes the energy of initial state. Note that, the intended prey is physically flagging in the case of $E_0 \in [-1, 0]$, whilst when the value of $E_0 \in [0, 1]$, it means that the intended prey is strengthening. t is the current iteration counter. And T represents the max iteration.

Different values of E establish the basis for a transition from exploration to exploitation smoothly, and determine the unique exploitative behaviors in the process of chasing intended prey. The hawks search the promising region in the case of $|E| \geq 1$, which is also known as exploration stage. On the contrary, when the value of escaping energy $|E| < 1$, the hawks are in the step of exploitation.

C. EXPLOITATION PHASE

When the hawks carry out "surprise pounce" strategy, the intended rabbit will try to rush to the safety instinctively. Hence, the exploitation phase is consisted of four models with respect to the escaping behaviors and chasing tactics of the hawks. Assume that r is a random number ranged from 0 to 1, where if $r < 0.5$ then the rabbit successfully escapes from dangerous situations; otherwise, the result is failure of escape. And the retained escaping energy $|E|$ is utilized to determine that the besiege is soft or hard.

1) SOFT BESIEGE

Although the rabbit has enough energy, but it does not succeed in escaping from attack due to some random misleading jumps in the case of $r \geq 0.5$ and $|E| \geq 0.5$. Moreover the hawks encircle the rabbit from different directions softly to make it more exhausted, and then conduct the surprise pounce. The behavior of hawks is modeled as follows:

$$X(t+1) = \Delta X(t) - E\left|JX_{prey}(t) - X(t)\right| \quad (20)$$

$$\Delta X(t) = X_{prey}(t) - X(t) \quad (21)$$

where $\Delta X(t)$ defines the gap between the location of intended rabbit and the position of current hawk in iteration t. r_5 is a random number ranged from [0, 1], and $J = 2(1 - r_5)$, denotes the random jump strength of intended rabbit in the process of escaping, which can mimic the natural motions of rabbit by virtue of random change.

2) HARD BESIEGE

The rabbit is very exhausted, as well as has a low escaping energy in the case of $r \geq 0.5$ and $|E| < 0.5$. Therefore, the hawks pay almost no effort to encircle intended rabbit before the surprise pounce performed. Each hawk updates its current position using the following equation.

$$X(t+1) = X_{prey}(t) - E\left|\Delta X(t)\right| \quad (22)$$

3) SOFT BESIEGE WITH PROGRESSIVE RAPID DIVES

The intended rabbit has enough energy to escape from attack, and the hawks still construct a soft besiege in the case of $r < 0.5$ and $|E| \geq 0.5$. In addition, the levy flight, an optimal searching tactic for predators in non-destructive foraging conditions, is utilized to model the escaping patterns of rabbit and leapfrog movements of hawks mathematically and accurately in this situation. According to the real behaviors of hawks, [31] assume that hawks can progressively select the best possible dive toward the intended prey. In another word, the hawks compare the possible result of each move to detect that will is be a good dive or not, and then implement the following rules correspondingly. To be more specific, the position of hawk is updated by (23) if next position is better than the current. Otherwise, the hawks will perform team rapid dives based on levy flight which can enhance exploitation capacity using (24).

$$Y = X_{prey}(t) - E\left|JX_{prey}(t) - X(t)\right| \tag{23}$$

$$Z = Y + S \times LF(D) \tag{24}$$

where D denotes the dimension of search space. S represents random selected vector which are sized at $1 \times D$.

$$LF(x) = 0.01 \times \frac{\mu \times \sigma}{|\nu|^{\frac{1}{\beta}}} \tag{25}$$

where $\sigma = \left(\dfrac{\Gamma(1+\beta) \times sin\left(\frac{\pi\beta}{2}\right)}{\Gamma\left(\frac{1+\beta}{2}\right) \times \beta \times 2^{\left(\frac{\beta-1}{2}\right)}}\right)^{\frac{1}{\beta}}$

The tactics which formulates the position vector of hawks in the next iteration can be summarized as follows:

$$X(t+1) = \begin{cases} Y & if\ F(Y) < F(X(t)) \\ Z & if\ F(Z) < F(X(t)) \end{cases} \tag{26}$$

4) HARD BESIEGE WITH PROGRESSIVE RAPID DIVES

The intended rabbit has too low energy to escape in the case of $r < 0.5$ and $|E| < 0.5$, and the hawks perform a hard besiege at the same time. The strategy for updating the positions of hawks is similar to that in soft besiege with progressive rapid dives. Note that, the team members try to shrink the distance between their average location and the location of intended rabbit in this situation.

$$Y = X_{prey}(t) - E\left|JX_{prey}(t) - X_m(t)\right| \tag{27}$$

where $X_m(t)$ has been defined in (17).

$$Z = Y + S \times LF(D) \tag{28}$$

The rule for updating the positions of hawks in the hard besiege with progressive rapids dives can be performed as follows:

$$X(t+1) = \begin{cases} Y & if\ F(Y) < F(X(t)) \\ Z & if\ F(Z) < F(X(t)) \end{cases} \tag{29}$$

Pseudo code of Harris hawks optimization for multilevel thresholding is shown in Fig. 2.

Input: Number of search agents N, the number of iterations T, D-dimensional space
Output: Optimum location and their corresponding fitness function values
Initialize the position of hawks $X_i\ (i=1,2,\ldots,\ n)$.
  WHILE the end condition is not satisfied
  FOR $i = 1 : n$
  Calculate the objective function value of each hawks through the Eq. (10) or Eq. (14).
  Update the position of the intended prey X_{prey},
  END FOR
  FOR $i = 1 : n$
    Update the initial energy E_0, jump strength J
    Update the escaping energy E using Eq. (19).
  IF $|E| \geq 1$ Exploration phase
  IF $q = rand(\ ) < 0.5$
  Update position vector using Eq. (16)
  ELSE
  Update position vector using Eq. (17)
  END IF
  END IF
  IF $|E| < 1$ Exploitation phase
  IF $r \geq 0.5$ and $|E| \geq 0.5$ Soft besiege
  Update position vector using Eq. (20)
  ELSE IF $r \geq 0.5$ and $|E| < 0.5$ Hard besiege
  Update position vector using Eq. (22)
  ELSE IF $r < 0.5$ and $|E| \geq 0.5$
  Soft besiege with progressive rapid dives
  Update position vector using Eq. (26)
  ELSE IF $r < 0.5$ and $|E| < 0.5$
  Hard besiege with progressive rapid dives
  Update position vector using Eq. (29)
  END IF
  Check and correct the new positions based on the boundaries of variables
  END FOR
  END WHILE
Return X_{prey}, which represents the optimal values for multilevel thresholding segmentation.

FIGURE 2. Pseudo code of Harris hawks optimization for multilevel thresholding.

IV. THE PROPOSED METHOD (HHO-DE)

A. THE DIFFERENTIAL EVOLUTION

Differential evolution (DE) is a simple and effective technique for solving optimization problems. There are four main steps in DE algorithm, namely, initialization, mutation, crossover, and selection [35].

Step 1: Initialization

The population X with size N is generated in this stage.

$$x_{ij} = round\ (lb + ((ub - lb)\ .*\ (rand\ (N, D)))) \tag{30}$$

TABLE 1. Parameters of each algorithm.

Algorithm	Parameters setting
HHO [31]	Constant $\beta=1.5$; Random jump strength $J\in[0,2]$
DE[35]	Scaling factor=0.5; Crossover factor=0.9
SCA[36]	controlling parameter $r_1\in[0,2]$
BA[37]	Loudness=0.25; Factor updating pulse emission rate γ=0.95
HSO[38]	PAR(Pitch Adjustment Rate)=0.3; HMCR(Harmony Memory Considering Rate)=0.95
PSO [39]	Learning factors c_1=$c_2=2$,Maximum velocity=25.5
DA[41]	Constant $\beta=0.5$

where *ub* and *lb* are the upper and lower bound of search space respectively. *D* denotes the dimension of search space.

Step 2: Mutation

The mutation operation is a crucial step for DE algorithm. For each target vector x_i^t $(i=1,2,\cdots N)$, a mutant vector V_i is generated by a mutation procedure, which can be formulated as follows:

$$V_i^t = x_{r_1}^t + SF * \left(x_{r_2}^t - x_{r_3}^t\right) \tag{31}$$

where *SF* represents the mutation scaling factor. r_1, r_2, and r_3 are distinct random integers belonging to $[1, N]$ and they cannot be equal.

Step 3: Crossover

The crossover operation can strengthen the diversity of population, and the trial individuals are chosen by means of the following equation.

$$u_{ij}^t = \begin{cases} V_{ij}^t & if\ \eta < CR\ or\ j = rand\ (i) \\ x_{ij}^t & otherwise \end{cases} \tag{32}$$

where η is a random number ranged from 0 to 1. x_{ij}^t is the position of current individual, V_{ij}^t is the position of mutant individual. $CR \in [0, 1]$ denotes the crosser probability. *rand* (i) is a random integer generated from the range $[1, D]$ to ensure that at least one component in u_{ij}^t is provided by V_{ij}^t.

Step 4: Selection

After crossover, the trial vector u_{ij}^t is calculated by the objective function. Then the greedy selection operation is applied to choose the better individual between the trial individuals u_{ij}^t and the target individuals x_{ij}^t through the comparison of fitness function values, and the selected individuals can survive in the next generation. The following rule is performed in selection operation of DE algorithm for minimization problems.

$$x_i^{t+1} = \begin{cases} u_i^t & if\ fit\left(u_i^t\right) < fit\left(x_i^t\right) \\ x_i^t & otherwise \end{cases} \tag{33}$$

where *fit* represents the fitness function value of a given problem.

B. THE HYBRID ALGORITHM (HHO-DE)

The standard Harris hawks optimization is a simple and effective algorithm for solving practical engineering problems. But note that, each meta-heuristic algorithm is not perfect and cannot fit to handle all optimization problems. In order to give full play to the advantage of HHO and avoid its limitations to some extent, as well as provide an alternative method to solve the problems in multilevel color image thresholding segmentation, this paper proposed a hybrid algorithm combining HHO and DE. In addition, between-class variance and Kapur's entropy are used as objective functions which will be maximized to find the optimal thresholds.

The process of implementation as follows:

Step 1: Initialize the population *X* with a size of *N* using the *rand* function.

Step 2: For the sake of simplicity, a whole population with size *N* is divided into equal two subpopulations according to fitness function values. The former subpopulation from 1 to $\frac{N}{2}$ will be assigned to Harris hawks swarm, and the latter from $\frac{N}{2}+1$ to *N* will be assigned to DE algorithm.

Step 3: The HHO and DE algorithms perform in parallel to update the positions of each subpopulation.

Step 4: The two updated subpopulations are merged together to generate a new population, and the global solution is selected from it by the comparison of fitness function values.

Step 5: End the iteration process until satisfying the termination condition.

Note that, the flowchart of HHO-DE for finding the optimal threshold values is described in Fig. 3.

V. EXPERIMENTS

In this section, firstly, we present a brief description of the experimental setup associated with multilevel thresholding. Then we show the parameter values of each algorithm which are used in experiments. Finally, in order to compare the segmentation performance of the proposed algorithm with other algorithms, five indicators, the average fitness function values, STD, PSNR, FSIM, and SSIM, are introduced in this section.

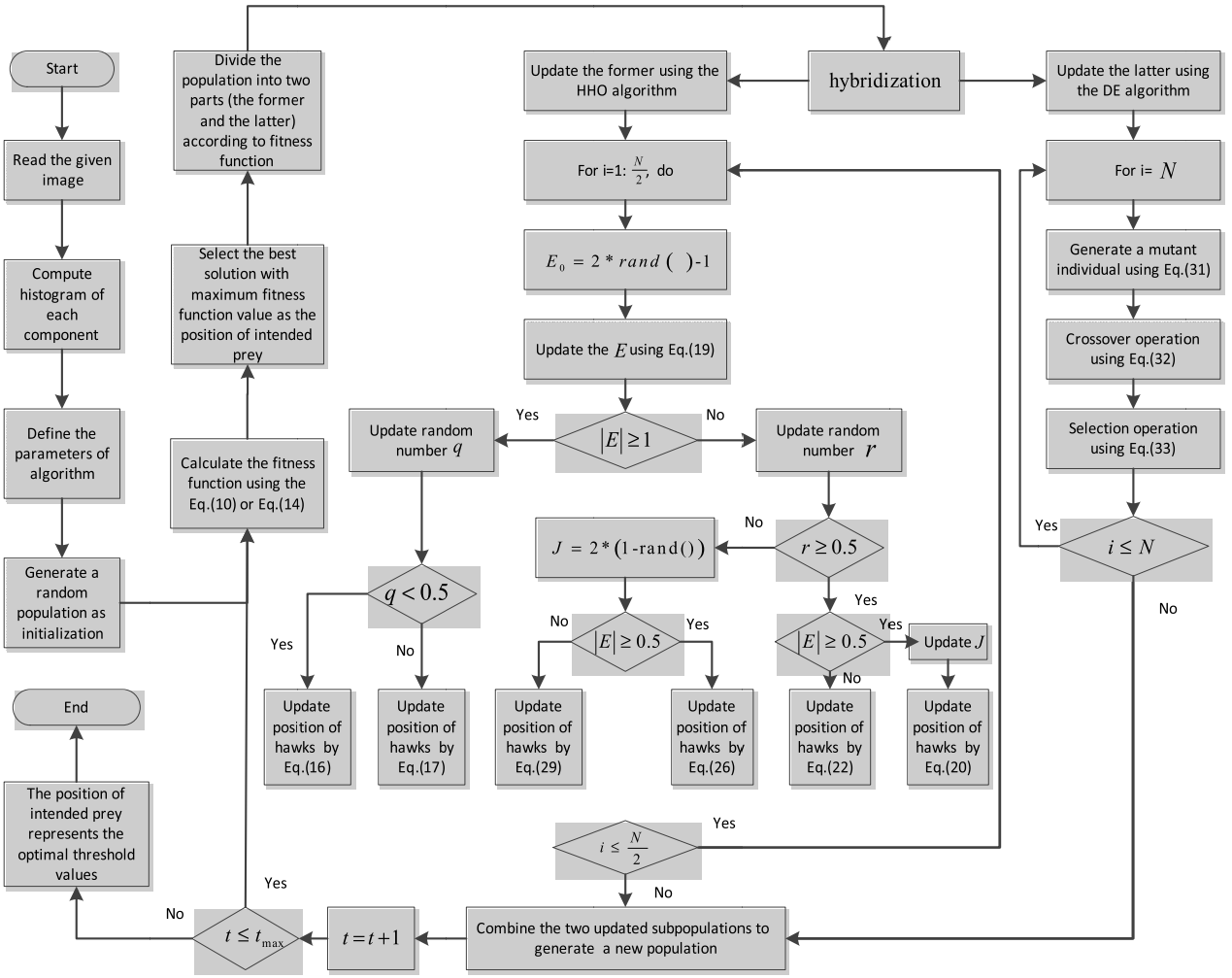

FIGURE 3. Framework of the OBLDA based method.

A. EXPERIMENTAL SETUP

In this paper, the proposed algorithm is tested on ten standard test images, namely Image1, Image2, Image3, Image4, Image5, Image6, Image7, Image8, Image9, and Image10, respectively. Images 1-5 are taken from the database of Berkeley University [44], which are of size 481 × 321, and satellite images 6-10 are taken from [45], which are also of size 481 × 321. Besides, all the test images and their corresponding histogram images are presented in Fig. 4. Performance of the proposed algorithm associated with Kapur's entropy and Otsu's method is compared with seven widely used optimization algorithms, namely, HHO, DE, SCA, BA, HSO, PSO, and DA algorithm. The SCA algorithm imitates the shock of sine and cosine functions to modify the candidate solutions and then converges to global optimum gradually. The BA algorithm is inspired from the echolocation behavior of bat. The HSO is a metaheuristic optimization algorithm inspired by the improvisation process of musicians. The PSO simulates the foraging behavior of birds or fishes in nature. The main inspiration of the DA algorithm is two different swarming behaviors of dragonflies, static and dynamic. All experiments are performed on the benchmark images with the following number of thresholds:4, 6, 8, 10, and 12.

B. PARAMETER SETTING

As we know, the value of parameters are of significance in determining the performance of each algorithm. In this paper, all algorithms have the same stopping conditions for a fair comparison. The max iteration is set to be 500 with a total of 30 runs each algorithm, and the population size is set to be 30. The specific parameters of each algorithm are presented in Table 1.

All the algorithms are developed by using "Matlab 2014b" and implemented on "Windows 10-64bit" environment on a computer having Pentium(R) Dual core T4500 @ 2.30 GHz and 2 GB of memory.

C. COMPARISON METRICS

This subsection introduces average fitness function, STD, PSNR, SSIM, and FSIM respectively, which will be applied in quantitative analysis of each algorithm.

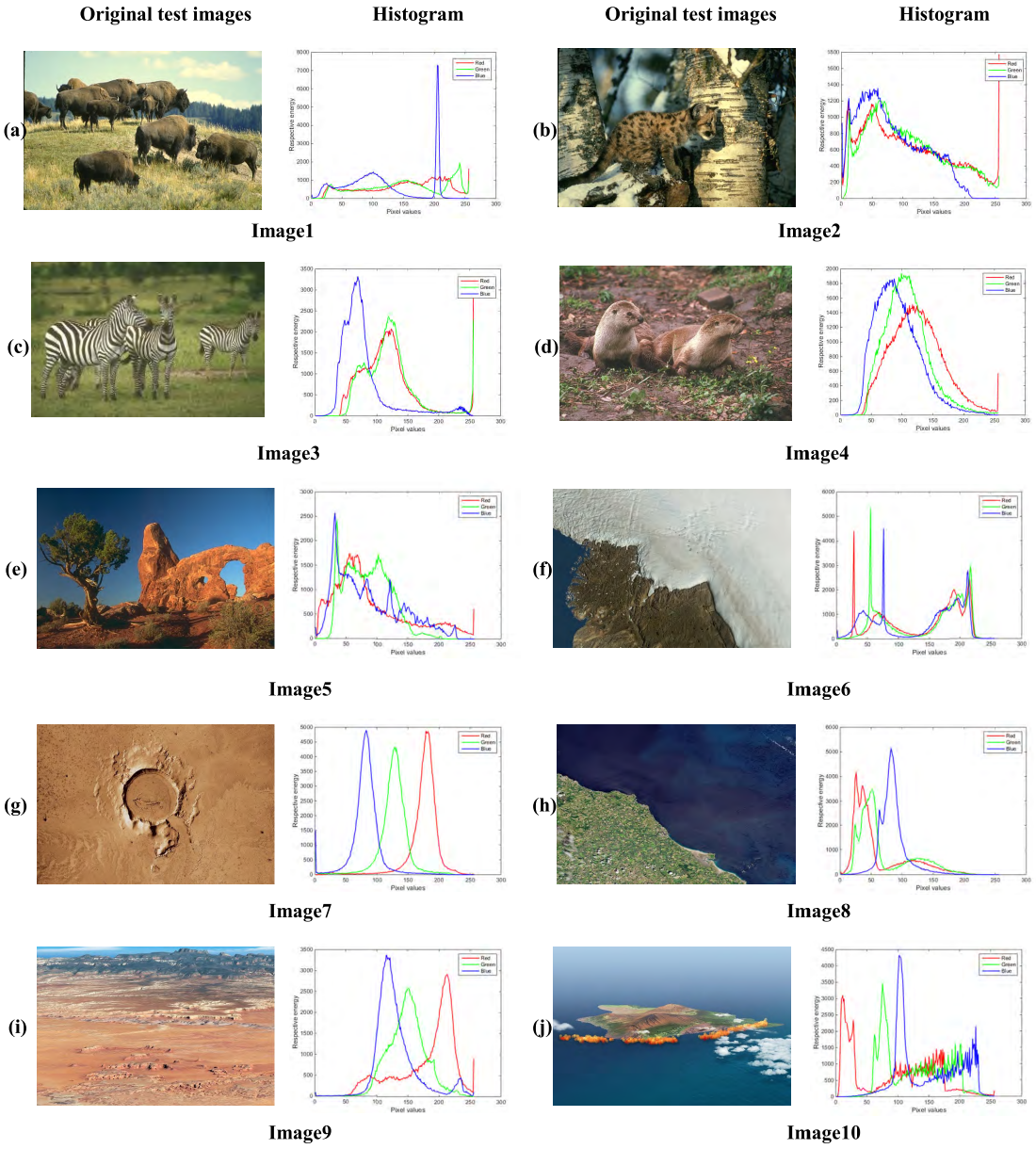

FIGURE 4. Original test images and the corresponding histograms for each of color channel.

1) THE AVERAGE FITNESS FUNCTION VALUES BY (10) OR (14)

2) THE STANDARD DEVIATION (STD)

Measure of how far a given variable is from the mean, which is used to evaluate stability. A lower value of STD indicates that the method is more stable.

$$STD = \sqrt{\frac{1}{n-1}\sum_{i=1}^{n}\left(f_i - \overline{f}\right)^2} \tag{34}$$

3) THE PEAK SIGNAL-TO-NOISE RATIO (PSNR)

The parameter of PSNR based on the produced mean square error (MSE) is used to verify the difference of the original image and segmented image [46]–[48], and the value refers to the quality of the segmented image. The PSNR is evaluated by:

$$PSNR = 10\log_{10}\left(\frac{255^2}{MSE}\right) \tag{35}$$

where

$$MSE = \frac{1}{MN}\sum_{i=1}^{M}\sum_{j=1}^{N}\left[I\left(i,j\right) - K\left(i,j\right)\right]^2$$

where $I(i,j)$ and $K(i,j)$ are the original and segmented images which are of size $M \times N$.

4) THE STRUCTURE SIMILARITY INDEX (SSIM)

The SSIM index helps to access the structural similarity between the original and segmented image [49]. The SSIM

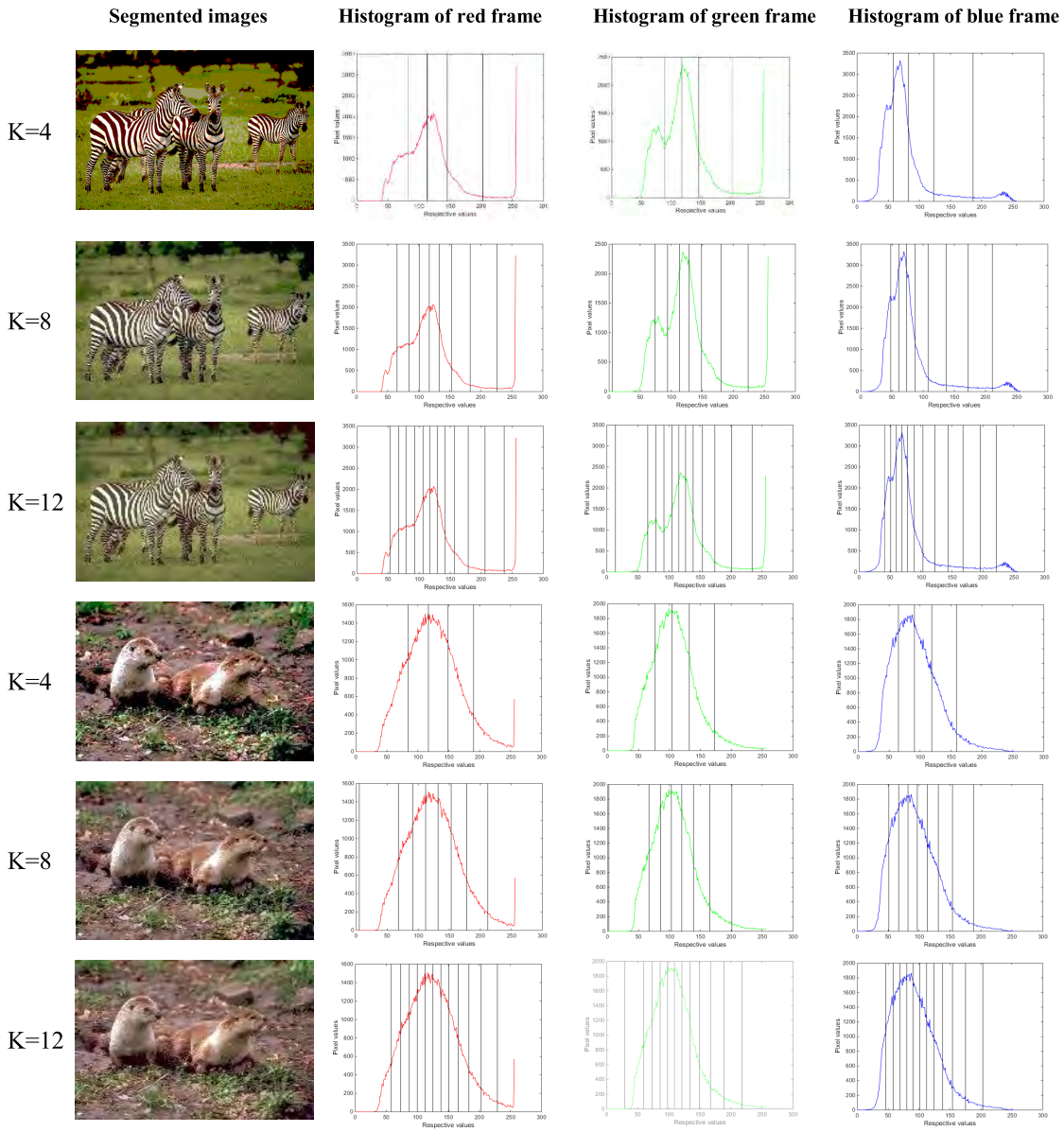

FIGURE 5. The segmented images of Image3 and Image4 using Otsu's method and each class shown by histograms for each of color channels.

is defined as:

$$SSIM\,(x,y) = [l\,(x,y)]^{\alpha}\,[c\,(x,y)]^{\beta}\,[s\,(x,y)]^{\gamma} \tag{36}$$

where, $l\,(x,y)$, $c\,(x,y)$, and $s\,(x,y)$ represent brightness comparison, contrast comparison, and structural information comparison function respectively. α, β, and γ are three parameters which are decided by the weight of the three parts. The functions are evaluated by

$$\begin{cases} l\,(x,y) = \dfrac{2\mu_x\mu_y + C_1}{\mu_x^2 + \mu_y^2 + C_1} \\ c\,(x,y) = \dfrac{2\sigma_x\sigma_y + C_2}{\sigma_x^2 + \sigma_y^2 + C_2} \\ s\,(x,y) = \dfrac{\sigma_{xy} + C_3}{\sigma_x\sigma_y + C_3} \end{cases} \tag{37}$$

where μ_x and μ_y represent the average intensity of the original and segmented images respectively. σ_x^2 and σ_y^2 represent the variance of the original and segmented images respectively. σ_{xy} is the covariance between the original and segmented images. C_1, C_2, and C_3 are set as follows: 6.5025, 58.5525, and 29.2613 respectively considering experiments of [50].

5) THE FEATURE SIMILARITY INDEX (FSIM)

A comparison of the features contained in the segmented image is performed using the FSIM and it is calculated as (31). The higher FSIM value indicates higher segmentation accuracy of the original image [51].

$$FSIM = \frac{\sum_{x\in\Omega} S_L\,(x) \times PC_m\,(x)}{\sum_{x\in\Omega} PC_m\,(x)} \tag{38}$$

TABLE 2. The average fitness values values of Otsu's method AND Kapur's ENTROPY in comparison with other algorithms.

Images	K	Otsu's method								Kapur's entropy							
		HHO-DE	HHO	DE	SCA	BA	HSO	PSO	DA	HHO-DE	HHO	DE	SCA	BA	HSO	PSO	DA
Image1	4	**3953.7954**	**3953.7954**	3953.7545	3948.8042	3953.6831	3953.3067	3953.7950	**3953.7954**	**18.5002**	18.5000	**18.5002**	18.4613	18.4966	18.4963	18.4932	18.5000
	6	**4018.8118**	4018.7966	4018.6085	4006.9266	4017.3416	4017.2234	4018.7985	4018.5048	**23.9812**	23.9607	23.9782	23.6436	23.8908	23.8975	23.9810	23.9799
	8	**4048.9289**	4048.8516	4046.2637	4024.1493	4037.8143	4045.3231	4043.3223	4048.8504	**28.8793**	28.8630	28.85 36	27.9375	28.5409	28.7200	28.7723	28.8129
	10	**4062.1226**	4061.9979	4060.0017	4039.0225	4050.5883	4059.3896	4061.1137	4063.1200	**33.4072**	33.251	33.3651	32.1934	31.8645	33.1194	33.1358	33.3523
	12	**4071.2558**	4071.2516	4069.2863	4054.429	4066.507	4069.2912	4070.6001	4070.1573	**37.5172**	37.4897	37.5097	35.7885	35.9101	37.2779	37.3461	37.4284
Image2	4	3485.1221	**3485.1247**	3485.0489	3479.1374	3484.6777	3484.7292	3485.1147	3485.1199	19.1177	**19.1179**	19.1165	19.1085	19.1174	19.1166	19.1185	19.1186
	6	**3569.8014**	3569.8000	3569.2589	3553.9263	3562.3733	3569.7989	3569.7922	3569.7975	**24.505**	24.5002	24.5048	24.3797	24.4700	24.4768	24.5045	24.5036
	8	**3604.7985**	3604.796	3602.9485	3576.8452	3583.8077	3600.4796	3604.6050	3604.7703	**29.2688**	29.2687	29.2685	28.6983	28.8901	29.1724	29.2628	29.2643
	10	**3622.7454**	3622.7334	3621.2069	3597.7083	3583.8832	3618.0966	3620.6747	3622.4558	**33.585**	33.5836	33.5718	32.2689	32.6558	33.4410	33.5548	33.5556
	12	**3633.0812**	3633.0709	3632.5519	3614.941	3612.3747	3626.1269	3630.7006	3630.5562	**37.5356**	37.5354	37.5298	34.4781	35.1123	37.1587	37.5247	37.5245
Image3	4	**1632.9348**	**1632.9348**	1632.9243	1629.3742	1632.8832	1632.5101	1632.9325	**1632.9348**	**17.9081**	17.9021	17.9076	17.8708	17.9068	17.8966	17.9080	17.9078
	6	**1679.6483**	1679.6434	1679.1492	1663.4943	1675.7384	1678.9156	1679.6217	1679.6224	**23.0198**	23.0135	23.0197	22.8565	22.9702	22.9593	23.0190	23.0113
	8	**1699.6865**	1696.9372	1699.3602	1677.6783	1694.3511	1697.2418	1696.9162	1699.6112	**27.6791**	27.6738	27.6623	26.8723	27.5156	27.5298	27.5934	27.6578
	10	**1709.8511**	1709.8467	1706.3519	1691.5336	1699.6933	1704.8673	1709.5613	1709.2274	**31.9448**	31.9441	31.9393	30.1086	30.4496	31.6635	31.8964	31.9280
	12	**1715.1719**	1714.8483	1713.5611	1700.6739	1706.4449	1709.738	1712.1207	1714.8516	**35.8441**	35.8418	35.8308	33.6783	34.7375	35.2639	35.7770	35.2063
Image4	4	1319.8912	1319.9467	1319.8154	1315.3303	1318.9811	1319.5916	**1319.9491**	1319.9489	18.4919	**18.4921**	18.4919	18.4622	18.4872	18.4819	18.4912	18.4916
	6	**1369.3151**	1361.021	1366.3527	1357.1484	1366.7841	1367.9945	1368.9969	1369.0213	**23.6966**	23.6934	23.6945	23.4468	23.6669	23.6125	23.6905	23.6914
	8	**1390.1987**	1390.1946	1385.5185	1374.3224	1389.2622	1387.4095	1387.4005	1390.0305	**28.3668**	28.3657	28.3553	27.9281	27.9847	28.2587	28.3067	28.3024
	10	**1401.0601**	1400.9161	1399.5777	1384.4908	1384.9509	1396.9234	1393.7362	1399.4009	**32.5966**	31.9136	32.5958	31.5723	31.3348	32.2579	32.5866	32.5865
	12	**1406.4562**	1406.2278	1406.4299	1384.8868	1393.2781	1401.2297	1404.5624	1405.6402	**36.4616**	36.4597	36.4545	35.5627	34.4852	35.9779	36.3520	36.3688
Image5	4	**2424.6317**	2424.5708	2424.4758	2421.2203	2424.5139	2424.2945	2424.5708	2424.5708	**18.7382**	18.7381	**18.7382**	18.6731	18.7217	18.7326	18.7372	18.7380
	6	**2487.0111**	2487.0034	2486.4827	2478.4116	2485.5045	2483.8617	2482.092	2480.7669	**24.0294**	24.0232	24.0187	23.6952	23.9584	24.0064	24.0237	24.0291
	8	**2512.4335**	2512.4307	2510.1776	2483.7068	2501.1752	2507.5583	2510.9344	2512.3053	**28.7447**	28.7442	28.7411	27.7347	28.2776	28.5286	28.7114	28.7079
	10	**2525.9419**	2525.9400	2522.0415	2501.6225	2509.8173	2520.1389	2519.899	2523.4752	**32.925**	32.9241	32.9206	30.6967	31.0099	32.6646	32.9146	32.9242
	12	**2533.3762**	2533.3685	2530.6872	2516.2091	2520.8127	2527.7053	2529.6907	2528.9949	**36.8556**	36.8234	36.8173	34.6304	34.6947	36.4877	36.0273	36.8009
Image6	4	**4106.9576**	**4106.9576**	4106.9412	4103.4725	4106.6185	4106.1335	4093.6918	4106.9548	**18.0763**	18.0402	18.0762	18.0206	18.0663	18.0625	**18.0763**	18.0762
	6	**4156.9731**	4156.9668	4155.6825	4144.5895	4149.1531	4156.1705	4156.7031	4156.9600	**23.2465**	23.2395	23.2409	23.0952	23.1252	23.1782	23.0487	23.2403
	8	**4177.3461**	4174.6103	4176.1387	4163.0824	4155.2176	4175.5775	4173.422	4177.0065	**27.9533**	27.866	27.9437	26.9866	27.2179	27.8200	27.9443	27.8775
	10	**4188.1996**	4188.197	4186.4405	4166.5066	4180.4813	4185.5519	4183.6386	4187.5649	**32.2359**	32.1942	32.2308	30.7732	29.9529	31.9572	32.1101	32.2195
	12	**4194.0612**	4193.2299	4192.4612	4180.0896	4184.6905	4189.9453	4192.7773	4193.6655	**36.2033**	36.1637	36.1887	33.7348	32.8871	35.7873	36.0606	36.1503
Image7	4	**485.58905**	**485.58905**	485.57167	482.36383	485.49969	484.82813	**485.58905**	**485.58905**	**17.9956**	17.9943	17.9932	17.9287	17.9733	17.9788	17.9951	17.9918
	6	**516.81265**	516.81377	516.66437	502.80496	515.94516	515.80145	516.77525	516.79802	**23.1194**	23.1143	23.1179	22.8755	23.0722	23.0877	23.0826	23.1104
	8	**529.72296**	529.70124	527.6709	518.34848	519.80773	523.23191	527.36023	529.58442	**27.789**	27.7872	27.7874	27.1359	27.4662	27.6283	27.7773	27.7665
	10	**536.35418**	536.35291	535.31066	521.15969	525.04284	531.61287	530.14982	535.96408	**32.0666**	32.0644	32.0661	30.8304	31.1550	31.8201	31.3980	32.0079
	12	**540.14973**	540.06596	539.60228	525.46624	529.16098	536.10605	536.14982	539.43856	**36.0202**	36.0148	36.0176	33.8099	34.1432	35.5297	35.9899	36.0040
Image8	4	**1434.3883**	**1434.3883**	1434.3504	1411.8967	1426.6895	1434.2426	1434.388	**1434.3883**	**18.6529**	**18.6529**	**18.6529**	18.6135	18.6235	18.6486	18.6513	18.6527
	6	**1465.7254**	1465.7123	1460.9474	1455.6995	1463.4165	1459.9255	1460.4346	1465.7107	**24.059**	23.9959	24.0029	23.6718	24.0132	24.0300	24.0136	24.0275
	8	**1479.8488**	1479.6576	1479.2531	1467.4106	1467.8256	1477.5762	1475.5254	1477.2392	**28.9563**	28.9519	28.8600	28.1968	28.5467	28.8082	28.9198	28.9500
	10	**1487.2432**	1487.105	1486.7208	1473.5682	1472.5074	1482.2186	1483.8691	1487.0162	**33.4995**	33.4699	33.4077	32.4014	32.1626	33.3038	33.3423	33.4139
	12	**1492.137**	1492.126	1491.2501	1481.1447	1479.6777	1487.5623	1488.6029	1491.3733	**37.6174**	37.6115	37.6073	37.0345	37.3708	37.3153	37.4806	37.5751
Image9	4	1278.0843	**1278.0851**	1278.064	1275.1557	1277.8696	1277.7294	1267.6957	1269.415	**18.6229**	18.6051	**18.6229**	18.5543	18.6166	18.5983	18.5973	18.5973
	6	**1319.4267**	1319.4300	1319.0548	1294.1183	1318.4037	1317.8799	1319.3821	1319.415	**24.1024**	24.1004	24.1004	23.2635	23.9888	24.0412	24.0716	24.0975
	8	**1338.3327**	1338.3054	1334.1936	1318.2704	1333.2169	1333.9997	1337.9987	1338.203	**28.9783**	28.9643	28.9729	28.6282	28.4515	28.2664	28.9739	28.9715
	10	**1347.5847**	1347.5396	1344.4151	1334.4783	1332.7321	1343.4454	1345.3956	1347.3194	**33.409**	33.4079	33.4019	31.0282	31.0731	32.1238	33.3761	33.3777
	12	**1353.1807**	1353.1205	1349.5096	1339.8847	1339.0017	1348.6086	1348.2386	1353.073	**37.5544**	37.5368	37.5153	35.4113	34.8624	37.2891	37.4450	37.4907
Image10	4	**2936.9941**	**2936.9941**	**2936.9941**	2921.8858	2916.7852	2916.2358	**2936.9941**	**2936.9941**	**18.3214**	18.2942	18.3213	18.2514	18.3088	18.0083	18.2762	18.3099
	6	**2979.7436**	2979.7034	2979.7267	2965.041	2965.3219	2977.0088	2967.1581	2979.7341	**23.8133**	23.7745	23.7821	23.5348	23.6608	23.7824	23.6999	23.8023
	8	**3000.1681**	3000.0721	3000.0346	2981.2949	2982.1163	2997.973	2999.7179	2999.5109	**28.6272**	28.5698	28.5021	27.7980	27.8766	28.5724	28.6210	28.5890
	10	**3011.4126**	3010.5281	3009.4417	2990.9484	2993.4874	3006.3938	3009.8252	3011.0473	**33.0156**	32.9738	33.0048	31.7141	30.6286	32.6996	32.9634	33.0064
	12	**3017.2308**	3017.1355	3015.4746	3000.0131	3003.2675	3016.900	3012.5378	3017.1636	**37.0185**	36.9149	36.9842	33.9013	33.8144	36.5600	36.9749	36.9573

where Ω represents the entire domain of the image. $PC_m(x)$ is defined as (39).

$$PC_m(x) = max\left(PC_1(x), PC_2(x)\right) \tag{39}$$

where, $PC_1(x)$ and $PC_2(x)$ represent the phase congruence of the original and segmented images, respectively.

The value of $S_L(x)$ is defined as follows:

$$S_L(x) = [S_{PC}(x)]^{\alpha} \cdot [S_G(x)]^{\beta} \tag{40}$$

where

$$S_{PC}(x) = \frac{2PC_1(x) \times PC_2(x) + T_1}{PC_1^2(x) \times PC_2^2(x) + T_1}$$

$$S_G(x) = \frac{2G_1(x) \times G_2(x) + T_2}{G_1^2(x) \times G_2^2(x) + T_2}$$

$S_{PC}(x)$ is the similarity of phase consistency between two images. $S_G(x)$ is the similarity of gradient magnitude between two images. $G_1(x)$ and $G_2(x)$ are the gradient magnitude of the original and segmented images, respectively. α, β, T_1 and T_2 are all constants.

VI. THE RESULTS AND DISCUSSIONS

This section presents the obtained results for proposed HHO-DE algorithm versus other algorithms based Otsu's method and Kapur's entropy, according to the average fitness function values, STD, PSNR, SSIM, and FSIM. Wilcoxon rank-sum test with 5% degree is also performed to see the significant difference between the proposed HHO-DE and other algorithms. And we compare the proposed method with super-pixel method in the end. All these are discussed at length in the following section.

Note that, the optimal threshold values (three color components: red, green, blue) at levels 4, 6, 8, 10, and 12 which obtained by all the algorithms more than 30 runs can be found in [52]. The segmented images of proposed HHO-DE algorithm and other algorithms with different threshold levels also can be found from [52]. Fig. 5. shows the distribution of occurrences in the classes. The black lines indicate the threshold values, and our aim is to determine the exact location of black lines indeed. Meanwhile, in order to easily and clearly observe and be convenient to visual analysis, the best results in tables briefly mentioned in the following section are highlighted in bold.

A. OBJECTIVE FUNCTION MEASURE

Otsu's method and Kapur's entropy are used as the objective function which will be maximized during optimization process. The average fitness function values of each algorithm

TABLE 3. The STD values of fitness functions using otsu's method in comparison with other algorithms.

Images	K	HHO-DE	HHO	DE	SCA	BA	HSO	PSO	DA
	4	**0.00E+00**	1.34E-01	1.28E-02	5.20E+00	1.65E-01	2.76E-01	6.79E-13	4.79E-13
	6	**1.54E-02**	2.32E-01	3.23E+00	6.04E+00	3.16E+00	6.97E-01	1.67E+00	1.56E-01
Image1	8	**1.89E-01**	3.40E-01	3.78E+00	5.15E+00	7.22E+00	1.09E+00	1.47E+00	1.71E+00
	10	**4.01E-01**	1.25E+00	1.42E+00	5.63E+00	5.25E+01	1.39E+00	5.58E-01	5.19E-01
	12	**4.31E-01**	5.79E-01	6.85E-01	4.62E+00	4.69E+00	9.86E-01	6.25E-01	8.05E-01
	4	1.05E-02	1.97E-02	5.28E+00	1.04E+00	1.09E-01	2.28E-01	**0.00E+00**	**0.00E+00**
	6	**6.70E-02**	9.00E-02	3.41E+00	4.89E+00	7.15E+00	6.90E-01	7.00E-02	7.39E-02
Image3	8	**1.12E-01**	3.15E-01	3.78E+00	5.67E+00	4.42E+00	1.43E+00	1.48E+00	2.50E-01
	10	**1.99E-01**	2.31E+00	1.86E+00	3.65E+00	4.48E+00	1.46E+00	5.03E-01	5.88E-01
	12	**5.42E-01**	7.93E-01	2.85E+00	5.12E+00	4.79E+00	8.04E-01	8.76E-01	8.42E-01
	4	**0.00E+00**	1.97E-02	5.28E+00	1.04E+00	1.09E-01	2.28E-01	**0.00E+00**	**0.00E+00**
	6	**6.70E-02**	9.00E-02	3.41E+00	4.89E+00	7.15E+00	6.90E-01	7.00E-02	7.39E-02
Image5	8	**1.12E-01**	3.15E-01	3.78E+00	5.67E+00	4.42E+00	1.43E+00	1.48E+00	2.50E-01
	10	**1.99E-01**	2.31E+00	1.86E+00	3.65E+00	4.48E+00	1.46E+00	5.03E-01	5.88E-01
	12	**5.42E-01**	7.93E-01	2.85E+00	5.12E+00	4.79E+00	8.04E-01	8.76E-01	8.42E-01
	4	**0.00E+00**	3.03E-02	5.19E+00	6.18E+00	4.43E-01	1.08E+00	2.39E-13	2.00E-13
	6	**2.56E-03**	1.78E-01	2.36E+00	4.89E+00	3.55E+00	4.80E-01	6.60E-03	5.60E-03
Image7	8	**2.42E-01**	2.54E-01	2.55E+00	5.79E+00	5.77E+00	8.57E-01	3.10E-01	5.02E-01
	10	**3.98E-01**	4.60E-01	1.02E+00	2.45E+00	4.78E+00	1.37E+00	3.94E-01	4.89E-01
	12	**5.01E-01**	6.71E-01	6.58E-01	6.99E+00	3.47E+00	9.63E-01	5.45E-01	7.12E-01
	4	**0.00E+00**	**0.00E+00**	2.78E-01	1.10E+00	1.05E-01	3.70E-01	2.04E-03	**0.00E+00**
	6	**2.09E-02**	2.83E-02	3.17E+00	2.89E+00	5.15E+00	1.16E+00	2.72E-02	2.21E-02
Image9	8	**1.96E-01**	2.16E-01	3.63E+00	3.46E+00	5.19E+00	6.60E-01	1.99E-01	2.01E-01
	10	**1.24E-01**	4.33E-01	1.99E+00	3.21E+00	4.89E+00	1.84E+00	3.58E-01	5.77E-01
	12	**2.32E-01**	2.72E-01	1.31E+00	2.66E+00	3.99E+00	8.92E-01	9.93E-01	1.18E+00

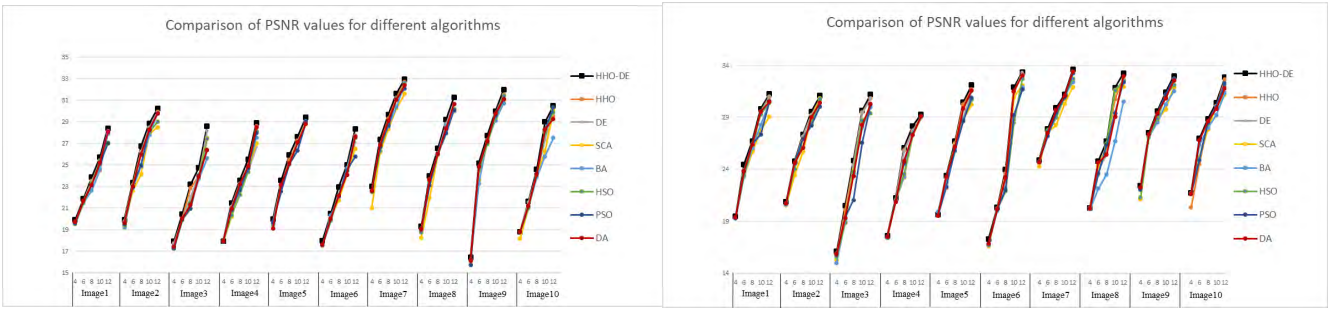

(a) (b)

FIGURE 6. Comparison of PSNR values obtained by all algorithms at K = 4,6,8,10, and 12. (a) PSNR—Otsu's method. (b) PSNR—Kapur's entropy.

are presented in Table. 2. In general, the higher value of average fitness function indicates better quality of solution. It is seen that the obtained results of proposed HHO-DE algorithm are the most outstanding, in almost all cases (47 out of 50 cases for Otsu's method and 48 out of 50 cases for Kapur's entropy). For example, the average fitness function values are 4177.3461, 4175.6103, 4175.6103, 4163.0824, 4155.2176, 4175.5775, 4173.422, and 4177.0065 for HHO-DE, HHO, DE, SCA, BA, HSO, PSO, and DA, respectively, when Image6 is tackled with 8 threshold levels using Otsu's method. Obviously, the average fitness function values of HHO-DE are highest and the DA algorithm is ranked second followed by HHO and DE, respectively. The results of experiment show that the proposed HHO-DE algorithm not only has advantage of tackling with extremum problems in multidimensional function, but also shows considerably strong engineering practicability in color image segmentation.

B. STABILITY ANALYSIS

The standard deviation with respect to average fitness function values is considered to verify the stability of proposed method. The lower the STD, the more stable of algorithm. Then the competitive results for 30 runs of HHO-DE and other algorithms are shown in Tables. 3-4. From the tables, it is found that the HHO-DE algorithm obtained the lowest values in 24 out of 25 cases (Otsu's method) and 23 out of 25 cases (Kapur's entropy). Therefore, it is evident that the HHO-DE algorithm has more remarkable stability than other algorithms.

TABLE 4. The STD values of fitness functions using Kapur's method in comparison with other algorithms.

Images	K	HHO-DE	HHO	DE	SCA	BA	HSO	PSO	DA
	4	**2.91E-05**	3.54E-05	6.46E-05	6.90E-03	1.10E-03	2.47E-02	3.95E-05	**2.91E-05**
	6	**2.38E-04**	4.63E-04	2.56E-04	3.11E-02	5.13E-02	3.29E-02	2.54E-04	7.19E-04
Image2	8	**2.19E-03**	5.67E-03	5.02E-03	2.00E-01	3.57E-01	3.09E-02	3.48E-03	4.16E-03
	10	**1.47E-02**	7.34E-02	3.05E-01	3.13E-01	4.78E-01	3.33E-02	1.50E-02	5.90E-02
	12	**2.66E-02**	2.98E-02	2.14E-01	5.89E-01	7.90E-01	6.60E-02	2.93E-02	2.85E-02
	4	2.78E-04	3.25E-04	8.64E-04	1.51E-02	1.10E-03	2.10E-02	5.76E-04	**0.00E+00**
	6	**1.06E-03**	1.10E-03	6.65E-03	3.49E-02	5.05E-02	1.48E-02	1.32E-02	1.47E-02
Image4	8	**2.07E-02**	2.13E-02	2.78E-02	2.51E-01	3.13E-01	6.36E-02	2.20E-02	3.03E-02
	10	**3.03E-02**	3.35E-02	2.02E-01	3.87E-01	5.34E-01	7.85E-02	3.16E-02	4.90E-02
	12	**3.89E-02**	4.33E-02	4.67E-01	5.08E-01	6.02E-01	5.47E-02	4.77E-02	5.96E-02
	4	**3.79E-04**	7.91E-03	1.56E-02	7.10E-03	3.30E-03	3.30E-03	1.10E-03	1.00E-03
	6	2.20E-03	3.81E-03	2.90E-03	3.35E-02	2.39E-02	1.24E-02	5.42E-04	**6.69E-04**
Image6	8	**5.30E-03**	1.20E-02	1.37E-02	1.99E-01	4.99E-01	2.19E-02	6.50E-03	7.00E-03
	10	**1.17E-02**	3.32E-02	1.20E-02	2.66E-01	7.42E-01	3.49E-02	3.50E-02	2.65E-02
	12	**3.10E-02**	4.60E-02	4.41E-02	3.53E-01	6.72E-01	8.23E-02	4.98E-02	4.51E-02
	4	**1.63E-04**	2.67E-04	1.78E-04	7.70E-03	1.23E-02	3.10E-03	5.45E-04	2.94E-04
	6	**1.30E-03**	4.80E-03	4.10E-03	6.47E-02	4.86E-02	1.22E-02	4.30E-03	2.90E-03
Image8	8	**1.80E-03**	1.89E-02	2.10E-03	1.85E-01	2.01E-01	3.68E-02	1.21E-02	1.94E-03
	10	**1.05E-02**	1.54E-02	1.27E-02	2.97E-01	3.42E-01	6.93E-02	3.45E-02	1.82E-02
	12	**2.15E-02**	3.33E-02	2.59E-02	3.55E-01	4.26E-01	3.25E-02	4.78E-02	2.67E-02
	4	**1.20E-03**	1.70E-03	**1.20E-03**	1.52E-02	2.90E-03	5.10E-03	**1.20E-03**	1.40E-03
	6	2.10E-03	2.30E-03	2.30E-03	5.66E-02	5.31E-02	2.21E-02	**1.80E-03**	2.30E-03
Image10	8	**5.60E-03**	6.04E-03	6.40E-03	9.58E-02	3.84E-01	1.61E-02	5.90E-03	6.10E-03
	10	**1.21E-03**	1.73E-02	5.60E-03	2.32E-01	4.98E-01	5.10E-02	2.88E-03	9.50E-03
	12	**2.11E-03**	2.29E-02	7.10E-03	4.32E-01	6.31E-01	6.29E-02	4.67E-03	1.77E-02

C. STATISTICAL ANALYSIS

A non-parametric statistical analysis based on Wilcoxon rand sum [41] is performed with a 5% significance level. The null hypothesis is defined as: there is no significant difference between the HHO-DE algorithm and seven other algorithms. And the alternative hypothesis considers a significant difference among them. The p-values are applicable to judge ''whether or not to reject the null hypothesis''. If p-value is greater than 0.05 and h = 0 simultaneously, the null hypothesis will be rejected, indicating there is no significant difference among all algorithms. On the contrary, the alternative hypothesis will be accepted at 5% significance level in which p is less than 0.05 or h = 1.

In order to prove the superiority of HHO-DE algorithm in a statistics way, each algorithm independently runs thirty times with a population of size thirty and five hundred iterations in tests for statistics analysis. All experimental data obtained based on Otsu's method and Kapur's entropy are used for testing. The results are shown in Table 5. The promising results indicate that the performance of HHO-DE algorithm has a remarkable improvement, and it is feasible and effective in the domain of multilevel thresholding color image segmentation

TABLE 5. Statistical analysis for the results.

Comparison	P-value(Otsu)	P-value(Kapur)
HHO-DE versus HHO	2.5389E-06	5.1569E-04
HHO-DE versus DE	1.4569E-06	8.5902E-05
HHO-DE versus SCA	2.4901E-08	3.7915E-06
HHO-DE versus BA	2.3762E-04	0.0015
HHO-DE versus HSO	6.3917E-05	6.1372E-05
HHO-DE versus PSO	4.7835E-06	1.0937E-05
HHO-DE versus DA	0.1003	0.0005

D. SEGMENTATION ACCURACY

In this section, we use PSNR, SSIM, and FSIM indicators to evaluate the segmentation accuracy of each algorithms. Meanwhile, in order to easily and clearly observe and be convenient to visual analysis, the line graphs of PSNR, SSIM, and FSIM are given in Figs. 6-8 respectively, including eight algorithms, ten images and five threshold levels. From these figures it can be seen that, the black lines with square data points which represents the proposed method are located above other lines for the majority cases. Note that, in order to make the structure more clear, we give the relevant experimental results in [52].

Firstly, the PSNR index which can compare the degree of image distortion is popular in image quality evaluation. A higher value of PSNR index indicates that the degree of image distortion is smaller. From the attained results, though there are only small differences between the proposed HHO-DE algorithm and other algorithms in the case of K = 4, the HHO-DE still shows superiority over the others to some extent (such as Images 3 and 6). For

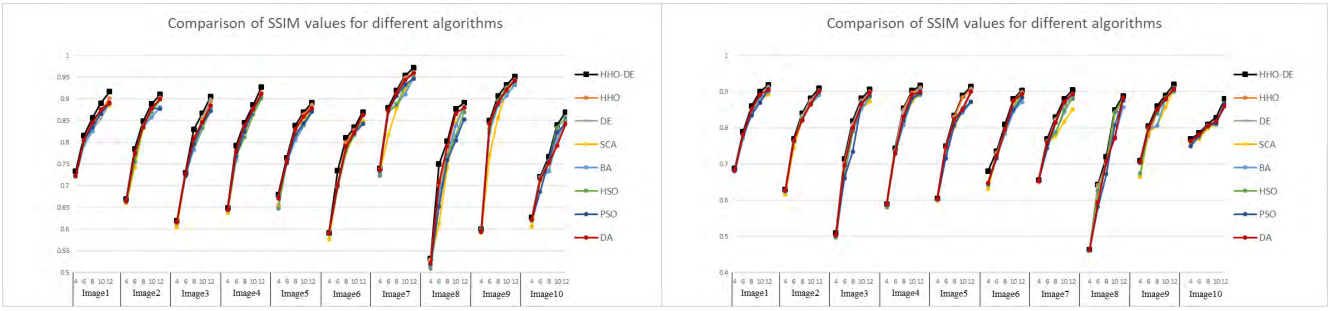

FIGURE 7. Comparison of SSIM values obtained by all algorithms at K = 4,6,8,10, and 12. (a) SSIM—Otsu's method. (b) SSIM—Kapur's entropy.

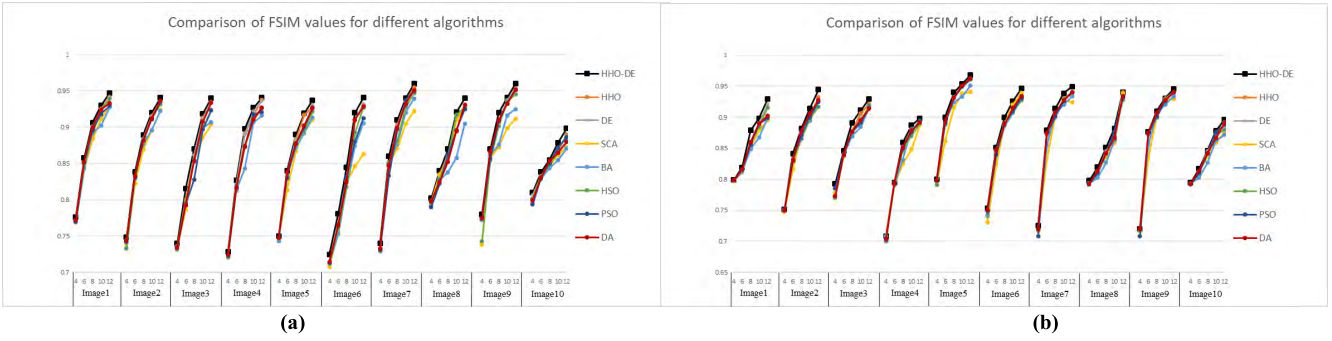

FIGURE 8. Comparison of FSIM values obtained by all algorithms at K = 4,6,8,10, and 12. (a) FSIM—Otsu's method. (b) FSIM—Kapur's entropy.

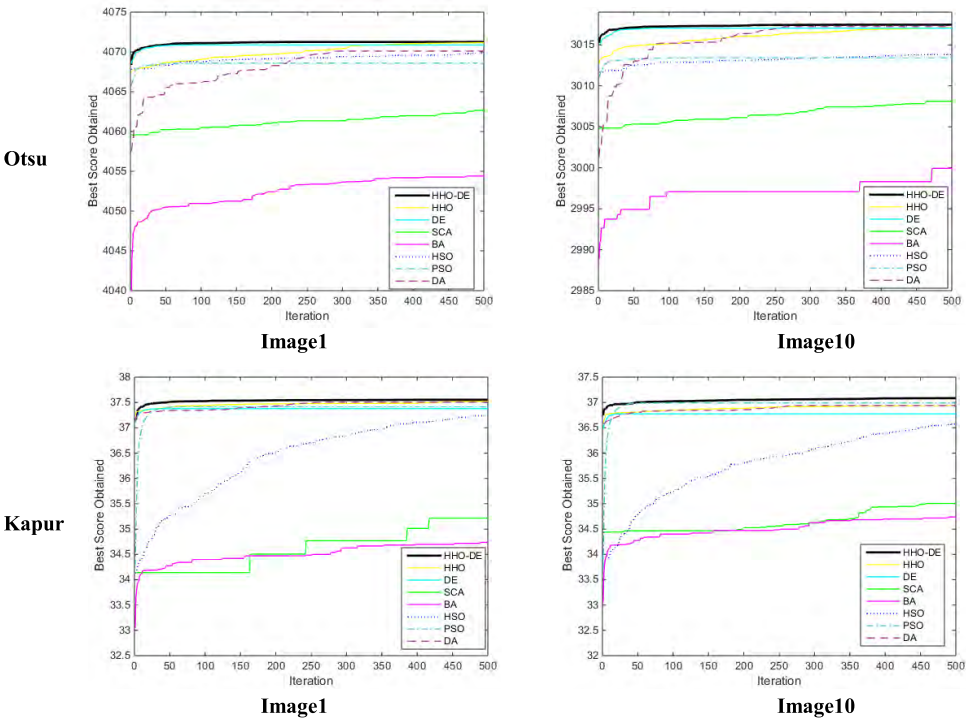

FIGURE 9. The convergence curves for average fitness function (30 independent runs) at 12 levels thresholding.

instance, the PSNR values are 17.2846, 16.8260, 16.8683, 16.6168, 16.7257, 16.7675, 16.8260, and 16.8489 for HHO-DE, HHO, DE, SCA, BA, HSO, PSO, and DA algorithm, respectively, when Kapur's method is applied on Image 6. What's more, the PSNR values of HHO-DE algorithm significantly increase by increasing the number of thresholds,

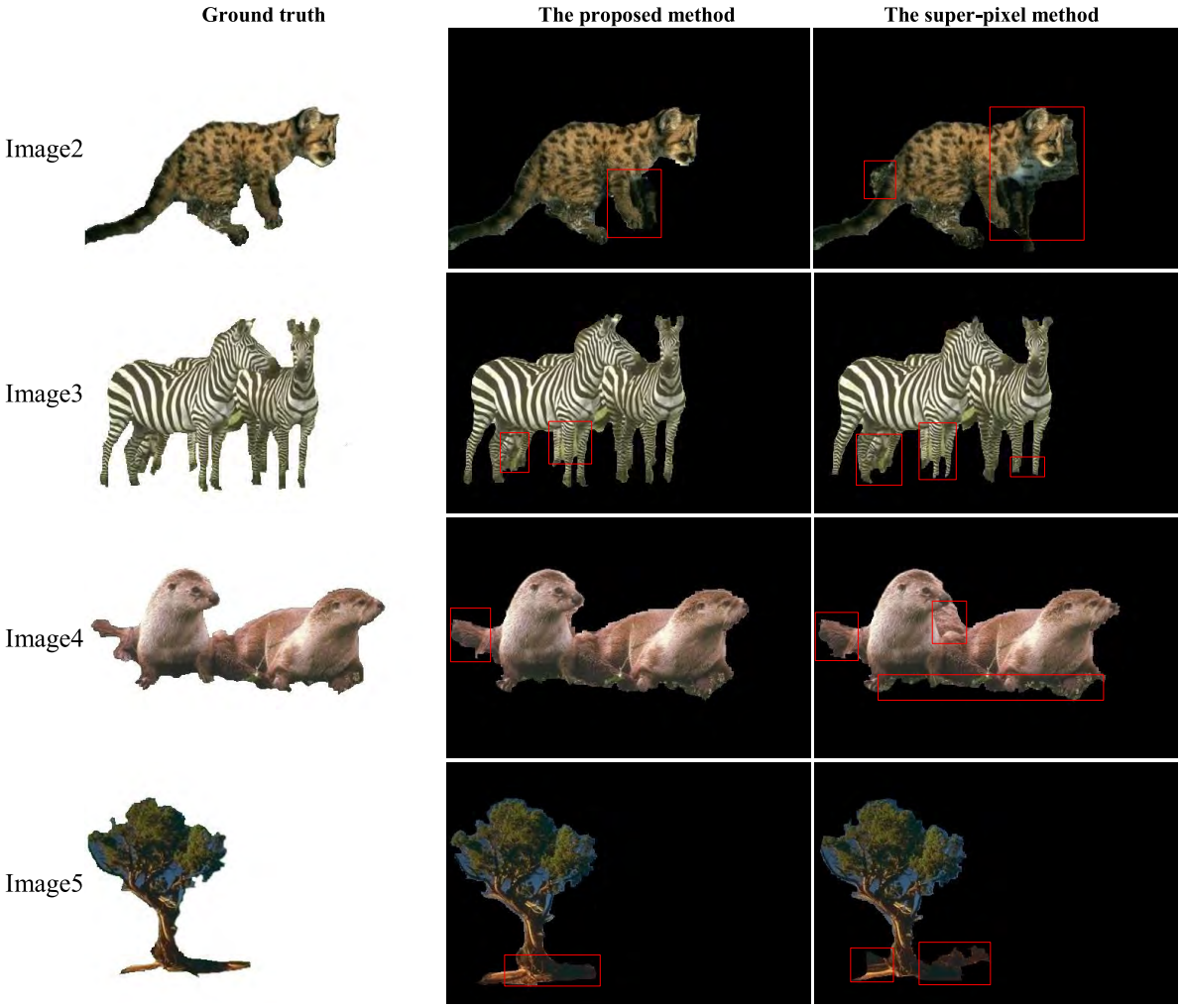

FIGURE 10. The segmented results and ground truth of test images.

so its merits are becoming more and more obvious. Therefore, the proposed HHO-DE algorithm based on Otsu's method and Kapur's entropy is superior to other algorithms in the performance of image segmentation.

Then, the SSIM index based on brightness, contrast and structural information is used to assess the visual similarity of the original image and the segmented image. A higher value of SSIM index indicates that the segmented image is more similarity to the original image. From the experimental results it is clearly observed that the proposed algorithm outperforms all the other algorithms, since the SSIM index obtains the highest values for majority of cases (48 out of 50 cases for Otsu's method and 49 out of 50 cases for Kapur's entropy). At the same time, as the number of thresholds increases, the value of SSIM continues to increase, as well as all algorithms can obtain more original image information. Hence, we can extract the interested objects more accurately, and the segmented images are more similar to the original images visually. For example, the SSIM values of Image 2 using Otsu's methods (HHO-DE) are 0.6805, 0.7857, 0.8364, 0.8798, and 0.9031 for the number of thresholds is 4, 6, 8, 10, 12, respectively, as a contrast, the SSIM values of Image 2 using Otsu's methods (DA) are 0.6775, 0.7754, 0.8354, 0.8788, and 0.9004 for the number of thresholds is 4, 6, 8, 10, and 12, respectively.

Last but not the least, the FSIM index associated with spatial gradient feature and phase consistency can distinguish the quality of segmented images. It can be seen from the results that, for the same image segmentation, the proposed algorithm obtains the most competitive results in almost all cases (49 out of 50 cases for Otsu's method and 48 out of 50 cases for Kapur's entropy). These values indicate that performance of the proposed algorithm is the most outstanding. For instance, the FSIM are for 0.9375, 0.9284, 0.9316, 0.9102, 0.9136, 0.9217, 0.9271, and 0.9264 for HHO-DE, HHO, DE, SCA, BA, HSO, PSO, and DA algorithm respectively, when Image5 is tackled with 12 threshold levels using Kapur's entropy. Hence, the interested targets can be extracted more accurately by proposed method for the majority of cases.

In summary, the results of experiments illustrated that the proposed HHO-DE algorithm using Otsu's method and Kapur's entropy can maintain a good balance between the exploratory and exploitative tendencies in the process of optimization. The performance of HHO-DE algorithm on color image segmentation with multilevel thresholding is satisfactory, because of high-quality and high-accuracy segmented images. Therefore, the proposed algorithm can be effectively applied in the field of color image segmentation

E. CONVERGENCE PERFORMANCE

The convergence curves of each algorithm using Otsu's technique and Kapur's entropy at 12 threshold levels are shown in Fig. 9. The progressively selection of HHO algorithm makes the search agents only select the better position, which may lead to lack enough global exploration ability to jump out of local optima. But with the hybridization of DE algorithm, the population diversity can be maintained in the late of optimization process and the convergence performance is satisfying. To enhance the validity of evaluation, the curves are obtained through calculating the average fitness function values of 30 independent runs. From the figures, it is detected that the HHO-DE algorithm has the most remarkable convergence property, and is capable of maintaining a good balance between exploratory and exploitative tendencies.

F. COMPARISON WITH SUPER-PIXEL METHOD

Super-pixel algorithm groups pixels of a given image into perceptually meaningful atomic regions, which can be used to replace the rigid structure of the pixel grid [53]. Image segmentation based on super-pixel is a completely different approach in comparison with Otsu's method or Kapur's entropy. It is used as a contrast method in this paper.

In order to fully demonstrate the effectiveness of the proposed HHO-DE method based multilevel thresholding algorithm, four test images, including Image 2, Image3, Image 4, and Image 5 are selected for experiments, and the segmented results are show in Fig. 10. Because there is no absolute standard for a given image, therefore we manually labeled the target region and separated it according to segmented results from Berkeley dataset. And then took it as the ground truth for experimental comparison. It can be found from the figures that the targets obtained by proposed method have been successfully separated from the complex background, which are similar to ground truth. By contrast, the targets obtained by super-pixel method has some defects. For example, the feet of zebra don't be separated obviously in Image3, and the tree roots cannot be distinguished from the rocks near them completely in Image5. To sum up, the proposed method can be considered as a competitive technique for multilevel color image segmentation.

VII. CONCLUSION

This paper presents an alternative method for multilevel thresholding color image segmentation inspired from the hybridization of HHO and DE algorithms. The contribution of proposed method is listed as follows: firstly, the validity and practicality of HHO in real-life optimization problems has been proved, hence, this paper makes creative use of HHO to enhance the performance of traditional multilevel threshold techniques. Secondly, due to the fact that each algorithm is not perfect, in order to give full play to its own advantages and overcome its own limitations to some extent, this paper combines the HHO and DE as a novel hybrid algorithm. Its merits include high accuracy, ability to avoid trapping into local optimum, remarkable stability and strong robustness. Otsu's method and Kapur's entropy are used as objective functions, which will be maximized in the process of searching for optimum thresholds. All experiments are performed on the ten benchmark images with the following number of thresholds: 4, 6, 8, 10, and 12. The performance of proposed algorithm are then compared with seven state-of-the-art algorithms, through the average fitness function values, STD, PSNR, SSIM, and FSIM indicators.

From the experimental results, it can be seen that there is a small gap between HHO-DE and other algorithms when realizing case with 4 threshold levels. But the competitive advantages resulted from HHO-DE algorithm are increasingly highlighted as the number of thresholds increases. The superior results obtained from PSNR, SSIM, and FSIM reveals that, the proposed method has high segmentation accuracy compared with other algorithms. The promising results of STD demonstrate that the remarkable stability of proposed method. In addition, Wilcoxon's rank-sum test with 5% degree also confirms the meaningful advantages of HHO-DE algorithm. Another merit of proposed method using Otsu's method and Kapur's entropy is the universality, to be more specific, it is not restricted to natural image, also shows satisfactory results in satellite image segmentation. Moreover, the comparison with super-pixel fully demonstrates the effectiveness of the proposed HHO-DE method based multilevel thresholding algorithm, Hence, the proposed method can accomplish real-world and complex task of multilevel thresholding color image segmentation excellently.

In future works, the proposed method can be employed to solve more practical engineering problems with superior performance. In addition, note that there is no technique which can adapt to all types of image segmentation. Thus, we will do our best to make further development in novel techniques for color image segmentation.

REFERENCES

[1] R. Manzke, C. Meyer, O. Ecabert, J. Peters, N. J. Noordhoek, A. Thiagalingam, V. Y. Reddy, R. C. Chan, and J. Weese, "Automatic segmentation of rotational X-ray images for anatomic intra-procedural surface generation in atrial fibrillation ablation procedures," *IEEE Trans. Med. Imag.*, vol. 29, no. 2, pp. 260–272, Feb. 2010.

[2] P. Qian, K. Zhao, Y. Jiang, K.-H. Su, Z. Deng, S. Wang, and R. F. Muzic, Jr., "Knowledge-leveraged transfer fuzzy *C*-means for texture image segmentation with self-adaptive cluster prototype matching," *Knowl.-Based Syst.*, vol. 130, pp. 33–50, Aug. 2017.

[3] A. Q. Yang, H. Huang, C. Zheng, X. Zhu, X. Yang, P. Chen, and Y. Xue, "High-accuracy image segmentation for lactating sows using a fully convolutional network," *Biosyst. Eng.*, vol. 176, pp. 36–47, Dec. 2018.

[4] Y. Yang, D. Tian, and B. Wu, "A fast and reliable noise-resistant medical image segmentation and bias field correction model," *Magn. Reson. Imag.*, vol. 54, pp. 15–31, Dec. 2018.

[5] S. Karimpouli and P. Tahmasebi, "Segmentation of digital rock images using deep convolutional autoencoder networks," *Comput. Geosci.*, vol. 126, pp. 142–150, May 2019.

[6] S. H. Lee, H. I. Koo, and N. I. Cho, "Image segmentation algorithms based on the machine learning of features," *Pattern Recognit. Lett.*, vol. 31, no. 14, pp. 2325–2336, Oct. 2010.

[7] F. Breve, "Interactive image segmentation using label propagation through complex networks," *Expert Syst. Appl.*, vol. 123, pp. 18–33, Jun. 2019.

[8] N. Tang, F. Zhou, Z. Gu, H. Zheng, Z. Yu, and B. Zheng, "Unsupervised pixel-wise classification for *Chaetoceros* image segmentation," *Neurocomputing*, vol. 318, pp. 261–270, Nov. 2018.

[9] S. Manikandan, K. Ramar, M. W. Iruthayarajan, and K. G. Srinivasagan, "Multilevel thresholding for segmentation of medical brain images using real coded genetic algorithm," *Measurement*, vol. 47, pp. 558–568, Jan. 2014.

[10] S. J. Mousavirad and H. Ebrahimpour-Komleh, "Multilevel image thresholding using entropy of histogram and recently developed population-based metaheuristic algorithms," *Evol. Intell.*, vol. 10, nos. 1–2, pp. 45–75, 2017.

[11] X. Fu, T. Liu, Z. Xiong, B. H. Smaill, M. K. Stiles, and J. Zhao, "Segmentation of histological images and fibrosis identification with a convolutional neural network," *Comput. Biol. Med.*, vol. 98, pp. 147–158, Jul. 2018.

[12] N. Otsu, "A threshold selection method from gray-level histograms," *IEEE Trans. Syst., Man, Cybern.*, vol. SMC-9, no. 1, pp. 62–66, Jan. 1979.

[13] J. N. Kapur, P. K. Sahoo, and A. K. C. Wong, "A new method for gray-level picture thresholding using the entropy of the histogram," *Comput. Vis., Graph., Image Process.*, vol. 29, no. 3, pp. 273–285, 1985.

[14] J. Li, W. Tang, J. Wang, and X. Zhang, "A multilevel color image thresholding scheme based on minimum cross entropy and alternating direction method of multipliers," *Optik*, vol. 183, pp. 30–37, Apr. 2019.

[15] S. Pare, A. K. Bhandari, A. Kumar, and G. K. Singh, "A new technique for multilevel color image thresholding based on modified fuzzy entropy and Lévy flight firefly algorithm," *Comput. Elect. Eng.*, vol. 70, pp. 476–495, Aug. 2018.

[16] A. K. Bhandari, A. Kumar, and G. K. Singh, "Tsallis entropy based multilevel thresholding for colored satellite image segmentation using evolutionary algorithms," *Expert Syst. Appl.*, vol. 42, no. 22, pp. 8707–8730, Dec. 2015.

[17] Y. Jiang, P. Tsai, W.-C. Yeh, and L. B. Cao, "A honey-bee-mating based algorithm for multilevel image segmentation using Bayesian theorem," *Appl. Soft Comput.*, vol. 52, pp. 1181–1190, Mar. 2017.

[18] A. R. J. Fredo, R. S. Abilash, and C. S. Kumar, "Segmentation and analysis of damages in composite images using multi-level threshold methods and geometrical features," *Measurement*, vol. 100, pp. 270–278, Mar. 2017.

[19] Y. Pan, Y. Xia, T. Zhou, and M. Fulham, "Cell image segmentation using bacterial foraging optimization," *Appl. Soft Comput.*, vol. 58, pp. 770–782, Sep. 2017.

[20] S. Pare, A. Kumar, V. Bajaj, and G. K. Singh, "An efficient method for multilevel color image thresholding using cuckoo search algorithm based on minimum cross entropy," *Appl. Soft Comput.*, vol. 61, pp. 570–592, Dec. 2017.

[21] R. Monisha, R. Mrinalini, M. N. Britto, R. Ramakrishnan, and V. Rajinikanth, "Social group optimization and Shannon's function-based RGB image multi-level thresholding," in *Smart Intelligent Computing and Applications*. Singapore: Springer, 2018. doi: 10.1007/978-981-13-1927-3_13.

[22] D. Guha, P. K. Roy, and S. Banerjee, "Optimal tuning of 3 degree-of-freedom proportional-integral-derivative controller for hybrid distributed power system using dragonfly algorithm," *Comput. Elect. Eng.*, vol. 72, pp. 137–153, Nov. 2018.

[23] G. Xiong, J. Zhang, D. Shi, and Y. He, "Parameter extraction of solar photovoltaic models using an improved whale optimization algorithm," *Energy Convers. Manage.*, vol. 174, pp. 388–405, Oct. 2018.

[24] G. G. Wang, "Moth search algorithm: A bio-inspired metaheuristic algorithm for global optimization problems," *Memetic Comput.*, vol. 10, pp. 151–164, Sep. 2018.

[25] L. He and S. Huang, "Modified firefly algorithm based multilevel thresholding for color image segmentation," *Neurocomputing*, vol. 240, pp. 152–174, May 2017.

[26] A. K. M. Khairuzzaman and S. Chaudhury, "Multilevel thresholding using grey wolf optimizer for image segmentation," *Expert Syst. Appl.*, vol. 86, pp. 64–76, Nov. 2017.

[27] L. Shen, C. Fan, and X. Huang, "Multi-level image thresholding using modified flower pollination algorithm," *IEEE Access*, vol. 6, pp. 30508–30519, 2018.

[28] B. Farnad, A. Jafarian, and D. Baleanu, "A new hybrid algorithm for continuous optimization problem," *Appl. Math. Modell.*, vol. 55, pp. 652–673, Mar. 2018.

[29] G. Sun, A. Zhang, Y. Yao, and Z. Wang, "A novel hybrid algorithm of gravitational search algorithm with genetic algorithm for multi-level thresholding," *Appl. Soft Comput.*, vol. 46, pp. 703–730, Sep. 2016.

[30] A. A. Ewees, M. A. Elaziz, and E. H. Houssein, "Improved grasshopper optimization algorithm using opposition-based learning," *Expert Syst. Appl.*, vol. 112, pp. 156–172, Dec. 2018.

[31] A. A. Heidari, S. Mirjalili, H. Faris, I. Aljarah, M. Mafarja, and H. Chen, "Harris hawks optimization: Algorithm and applications," *Future Gener. Comput. Syst.*, vol. 97, pp. 849–872, Aug. 2019.

[32] Q. Guo and L. Tang, "Modelling and discrete differential evolution algorithm for order rescheduling problem in steel industry," *Comput. Ind. Eng.*, vol. 130, pp. 586–596, Apr. 2019.

[33] E. G. Martinez-Soltero and J. Hernandez-Barragan, "Robot navigation based on differential evolution," *IFAC-PapersOnLine*, vol. 51, no. 13, pp. 350–354, 2018.

[34] H. R. Chamorro, I. Riano, R. Gerndt, I. Zelinka, F. Gonzalez-Longatt, and V. K. Sood, "Synthetic inertia control based on fuzzy adaptive differential evolution," *Int. J. Elect. Power Energy Syst.*, vol. 105, pp. 803–813, Feb. 2019.

[35] U. Mlakar, B. Potočnik, and J. Brest, "A hybrid differential evolution for optimal multilevel image thresholding," *Expert Syst. Appl.*, vol. 65, pp. 221–232, Dec. 2016.

[36] S. Mirjalili, "SCA: A sine cosine algorithm for solving optimization problems," *Knowl.-Based Syst.*, vol. 96, pp. 120–133, Mar. 2016.

[37] M.-H. Horng, "A multilevel image thresholding using the honey bee mating optimization," *Appl. Math. Comput.*, vol. 215, no. 9, pp. 3302–3310, Jan. 2010.

[38] M. J. Hadidian-Moghaddam, S. Arabi-Nowdeh, M. Bigdeli, and D. Azizian, "A multi-objective optimal sizing and siting of distributed generation using ant lion optimization technique," *Ain Shams Eng. J.*, vol. 9, pp. 2101–2109, Dec. 2018.

[39] T. X. Pham, P. Siarry, and H. Oulhadj, "Integrating fuzzy entropy clustering with an improved PSO for MRI brain image segmentation," *Appl. Soft Comput.*, vol. 65, pp. 230–242, Apr. 2018.

[40] R. K. Sambandam and S. Jayaraman, "Self-adaptive dragonfly based optimal thresholding for multilevel segmentation of digital images," *J. King Saud Univ.-Comput. Inf. Sci.*, vol. 30, no. 4, pp. 449–461, Oct. 2018.

[41] F. Wilcoxon, "Individual comparison by ranking methods," *Biometrics Bolletin*, vol. 1, no. 6, pp. 80–83, Dec. 1945.

[42] S. J. Mousavirad and H. Ebrahimpour-Komleh, "Entropy based optimal multilevel thresholding using cuckoo optimization algorithm," in *Proc. 11th Int. Conf. Innov. Inf. Technol. (IIT)*, Nov. 2015, pp. 302–307. doi: 10.1109/INNOVATIONS.2015.7381558.

[43] A. K. Bhandari, V. K. Singh, A. Kumar, and G. K. Singh, "Cuckoo search algorithm and wind driven optimization based study of satellite image segmentation for multilevel thresholding using Kapur's entropy," *Expert Syst. Appl.*, vol. 41, no. 7, pp. 3538–3560, Jun. 2014.

[44] *The Berkeley Segmentation Dataset and Benchmark*.Accessed: Dec. 15, 2018. [Online]. Available: https://www2.eecs.berkeley.edu/Research/Projects/CS/vision/grouping/segbench/BSDS300/html/dataset/images.html

[45] *Landsat Imagery Courtesy of NASA Goddard Space Flight Center and U.S. Geological Survey*. Accessed: Jan. 27, 2019. [Online]. Available: https://landsat.visibleearth.nasa.gov/index.php?&p=1

[46] A. Aldahdooh, E. Masala, G. Van Wallendael, and M. Barkowsky, "Framework for reproducible objective video quality research with case study on PSNR implementations," *Digit. Signal Process.*, vol. 77, pp. 195–206, Jun. 2018.

[47] S. J. Mousavirad and H. Ebrahimpour-Komleh, "Human mental search-based multilevel thresholding for image segmentation," *Appl. Soft Comput.*, to be published. doi: 10.1016/j.asoc.2019.04.002.

[48] A. K. Bhandari, "A novel beta differential evolution algorithm-based fast multilevel thresholding for color image segmentation," *Neural Comput. Appl*, pp. 1–31, Oct. 2018. doi: 10.1007/s00521-018-3771-z.

[49] J. John, M. S. Nair, P. R. A. Kumar, and M. Wilscy, "A novel approach for detection and delineation of cell nuclei using feature similarity index measure," *Biocybern. Biomed. Eng.*, vol. 36, no. 1, pp. 76–88, Aug. 2016.
[50] Z. Wang, A. C. Bovik, H. R. Sheikh, and E. P. Simoncelli, "Image quality assessment: From error visibility to structural similarity," *IEEE Trans. Image Process.*, vol. 13, no. 4, pp. 600–612, Apr. 2004.
[51] K. S. Beevi, M. S. Nair, and G. R. Bindu, "Automatic segmentation of cell nuclei using Krill Herd optimization based multi-thresholding and localized active contour model," *Biocybern. Biomed. Eng.*, vol. 36, no. 4, pp. 584–596, 2016.
[52] *A Novel Hybrid Harris Hawks Optimization for Color Image Multilevel Thresholding Segmentation*. Accessed: Apr. 30, 2019. [Online]. Available: https://github.com/baoxiaoxue/HHO-DE/blob/master/data-A-Novel-Hybrid-Harris-Hawks-Optimization-for-Color-Image-Multilevel-Thresholding-Segmentation.pdf
[53] R. Achanta, A. Shaji, K. Smith, A. Lucchi, P. Fua, and S. Süsstrunk, "SLIC superpixels compared to state-of-the-art superpixel methods," *IEEE Trans. Pattern Anal. Mach. Intell.*, vol. 34, no. 11, pp. 2274–2282, Nov. 2011.

XIAOLI BAO was born in Dingzhou, China, in 1997. She is currently pursuing the B.S. degree in automation from Northeast Forestry University, China. Her research interests include image segmentation and swarm intelligence algorithm.

HEMING JIA received the Ph.D. degree in system engineering from Harbin Engineering University, China, in 2012. He is currently an Associate Professor with Northeast Forestry University. His research interests include nonlinear control theory and application, image segmentation, and swarm optimization algorithm.

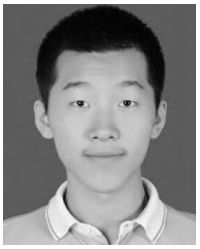

CHUNBO LANG was born in Shenyang, China, in 1998. He is currently pursuing the B.S. degree in automation from Northeast Forestry University, China. His research interests include image segmentation and swarm intelligence algorithm.